Pharmaceutical aspects of salt and cocrystal forms of APIs and characterization challenges

Pharmaceutical aspects of salt and cocrystal forms of APIs and characterization challenges

Paolo Cerreia Vioglio, Michele R. Chierotti, Roberto Gobetto*
Department of Chemistry, University of Torino, Via P. Giuria 7, 10125 Torino (Italy)

Contents

ABSTRACT

In recent years many efforts have been devoted to the screening and the study of new solid-state forms of old active pharmaceutical ingredients (APIs) with salification or co-crystallization processes, thus modulating final properties without changing the pharmacological nature. Salts, hydrates/solvates, and cocrystals are the common solid-state forms employed. They offer the intriguing possibility of exploring different pharmaceutical properties for a single API in the quest of enhancing the final drug product. New synthetic strategies and advanced characterization

techniques have been recently proposed in this hot topic for pharmaceutical companies. This paper reviews the recent progresses in the field particularly focusing on the characterization challenges encountered when the nature of the solid-state form must be determined. The aim of this article is to offer the state-of-the-art on this subject in order to develop new insights and to promote cooperative efforts in the fascinating field of API salt and cocrystal forms.

1. Introduction

In the pharmaceutical industry, a major driving force leading to new technological developments is the enhancement of the essential properties of an active pharmaceutical ingredient (API) for instance solubility, bioavailability, flow properties, and thermal stability but also crystallinity, hygroscopicity, particle size, filterability, density, and taste are important. Thus, the improvement of a drug product brings in desirable benefits in terms of better, effective therapies and economic savings. This is a topic of broad and current interest, as the discovery of new drugs has suffered a setback due to the crisis the pharmaceutical companies are facing today in their R&D sector [1]. Moreover, it is estimated that more than 60% of new drug molecules display poor aqueous solubility, due to an increased size and lipophilicity [2]. Such difficulties have further prompted researchers to pursue other means of developing and improving pharmaceutical products, for example by exploring new solid-state forms of old APIs with salification or co-crystallization processes, thus modulating final properties without changing the pharmacological nature [3]. Hence, in recent years many efforts have been devoted to the screening and the study of multicomponent pharmaceutical forms, as they may possibly represent tomorrow's route to the preparation of drugs. In this context, polymorphs, salts, hydrates/solvates, and cocrystals are the common solid-state forms employed; each one may exhibit different pharmaceutical parameters for a single API, and finding the optimal solid-state form requires a broad screening during the early phase of drug development. From the viewpoint of manufacturability and stability, the most thermodynamically stable form should be selected appropriately for the development [4].

Historically, salts have long been the first choice for overcoming poor solubility and dissolution rate problems, whereas cocrystals have been the subject of intense research only in recent times [5–7]. Also polymorphs and amorphous solids have been widely used to optimize the efficacy and delivery [8]; however, they fall outside the scope of this review and will not be discussed here. Exceptions will be made in cases of salts or cocrystals exhibiting notable polymorphism.

Cocrystals expand the possibilities to explore new API forms, since they are not limited to ionizable drugs as in the case of salts; in fact, they can also be made for non-ionizable molecules. Furthermore, the number of cocrystal co-formers is in principle limited only by safety requirements (*i.e.*, safe for human consumption) and by the affinity between functional groups which interact through non-covalent bonds. An interesting sub-group of cocrystals is the one composed of charged cocrystal systems, namely salt cocrystals (SCCs) [9–11], ionic cocrystals (ICCs) [12–17], and zwitterionic cocrystals [18,19]. This approach aims to combine the unique features of a salt and an API in a single entity: the goal is to exploit the synergistic effect, thus yielding improved drug products or even drug-drug cocrystals [14]. Although cocrystals have not yet gained significant market share [20], prospects are promising indeed.

In terms of intellectual property, all new salt and cocrystal forms of APIs are considered patentable and they certainly represent a commercial opportunity [21]. Moreover, a new salt or cocrystal is

eligible for an extension of patent rights: the approval will also be simpler because of the existence of previous knowledge coming from the early pharmaceutical form [22].

The portfolio of API salt forms offers several strategies to alter the therapeutic significance of drugs, by changing their dissolution, absorption, and other physico-chemical and pharmacokinetic aspects [23–25]. It is noteworthy that the aims of new API salt forms research are mainly focused on improving the dissolution properties and consequently the absorption of drugs. This affects the bioavailability of the drug, and in certain cases it might lead to adverse effects for the patient [24]. Hence, the strategies for improving the bioavailability should also consider appropriate investigations to match the desired pharmacokinetic response or therapeutic effect.

As it appears from these brief pharmacological and regulatory considerations, it is important to distinguish among the various salt forms of API. The determination of whether a salt or a cocrystal has formed can be difficult, especially when poor quality single crystals are obtained for X-ray diffraction (XRD). Crystal structure determination often does not afford accurate proton positions, therefore other techniques are necessary. The empiric pK_a rule is highly debated in the community since pK_a is evaluated with respect to the solvent, usually water, and not in the solid state [26] and also depends on the temperature. It works well when the ΔpK_a ($pK_{a(base)} - pK_{a(acid)}$) is greater than 3, but when it comes to the 0–3 range (as it is usual in cocrystal synthesis) one must collect other evidences for distinguishing crystal forms. In this regard, several examples in the literature have already demonstrated, by using diffractometry, solid-state Nuclear Magnetic Resonance (SSNMR), quantum calculations, thermal analysis, vibrational spectroscopy and hot-stage microscopy, that the proton position does matter [27–32] and represents a hot topic for pharmaceutical companies.

The large number of structures encompassed by this classification makes it a formidable task to include all of them in the present article. This is intended to be an overview of some of the currently most promising pharmaceutical salt and cocrystal forms of APIs, with an emphasis on their characterization.

This review is organized as follows. In section 2 we examine the differences among the various API salt forms, from both a theoretical and pharmacological perspective; a description of common synthetic methods is also given in section 3. Section 4 will focus on the characterization challenges related to the proton position disclosing a large array of techniques able to provide insights on the neutral or ionic nature of the crystal forms. In the final section, section 5, we review some selected examples of the many reported in the literature, focusing on the challenges encountered when the nature of the solid-state form must be determined.

For the sake of clarity, the chemical structures of all API and coformer molecules cited in this article are represented in Schemes 1 and 2, respectively.

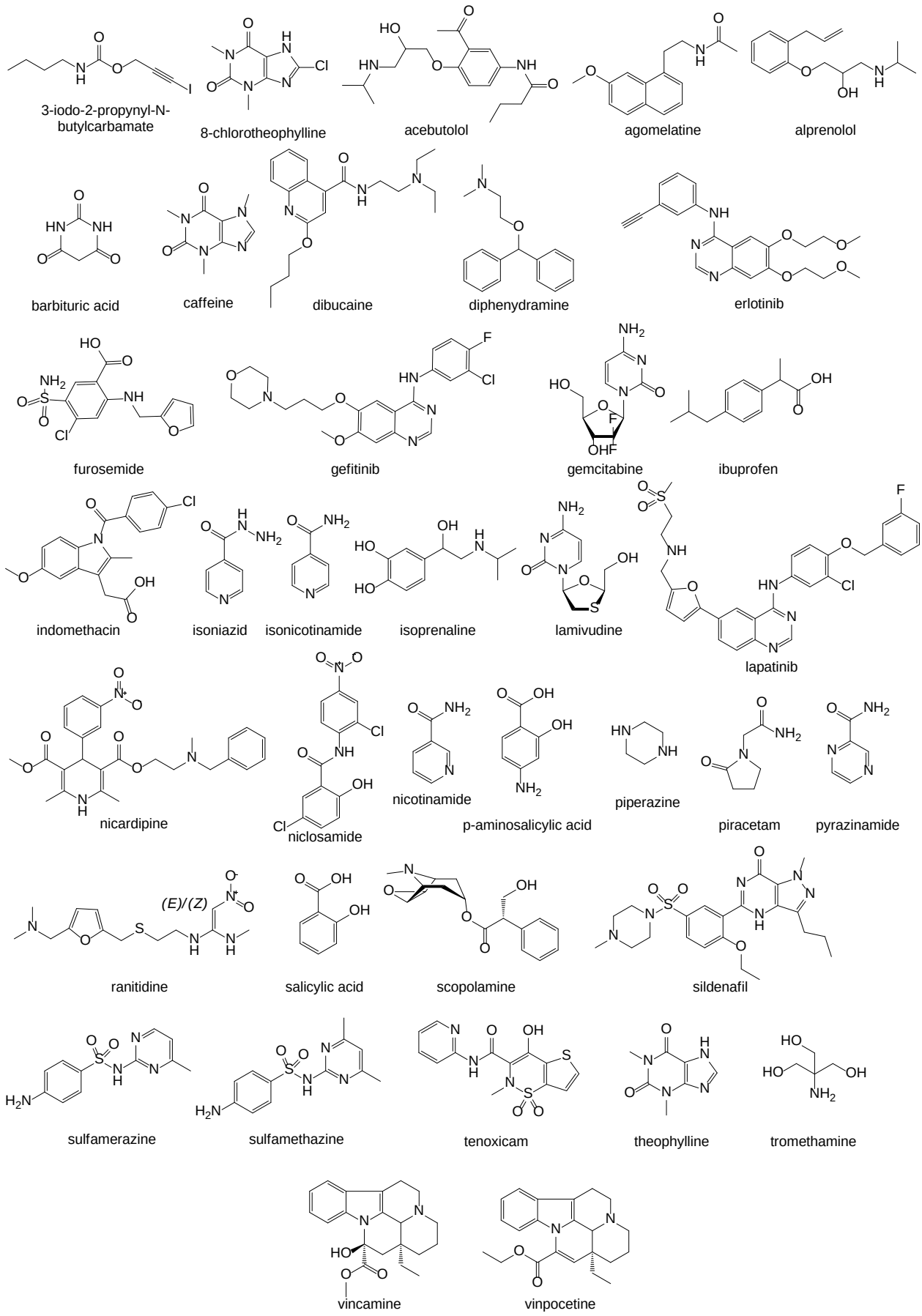

Scheme 1. Non-exhaustive list of APIs utilised to form salts and cocrystals.

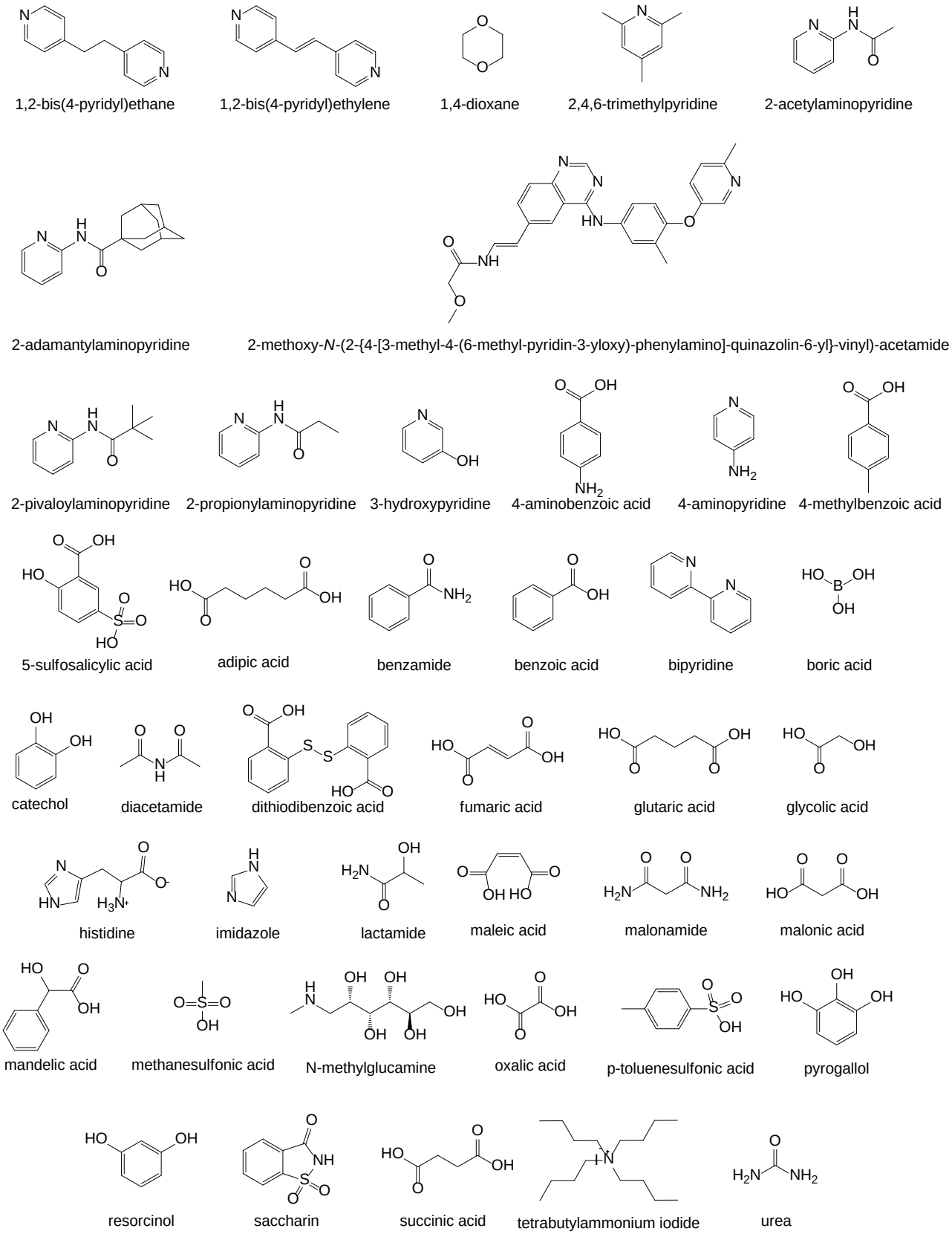

Scheme 2. Non-exhaustive list of coformers utilised to form pharmaceutical salts and cocrystals.

2. Definitions and general properties

Most APIs (65 to 70%) are administered in the solid form, and the crystalline state is preferred due to its relative ease of synthesis, the rejection of impurities, and the physico-chemical stability [25,33]. Crystal forms are advantageous in the quest of enhancing and optimizing drug products, and their design and synthesis is one of the most active areas of modern solid-state chemistry [34]. The whole set of notions and procedures to make crystals with a purpose has merged into what we now call *crystal engineering*. Crystal engineering may be viewed as a form of supramolecular synthesis, that is, "the chemistry beyond the molecule", and has already demonstrated to be able to contribute in developing pharmaceuticals and other functional materials (Fig. 1) [35–37]. Consequently, both the United States Food and Drug Administration (FDA) and the European Medicines Agency (EMA) have made attempts towards the regulatory classification of novel crystal forms [38], thus weighing in on the intense debate among scientists [27,39,40]. Some generally accepted definitions of salts, cocrystals, and their combinations are however available; we summarize them in the following paragraphs.

2.1 Salts

The salification of an API is the most common method to improve its aqueous solubility and bioavailability [5,41]. In the last 60 years, the pharmaceutical industry has increasingly used the salification process to enhance the properties of drug products, and today more than 50% of the drugs on the market are sold as salts [41,42]. The reasons for this success are the relative ease of synthesis and crystallization, and reliability of the product. Salt formation is not limited to the modification of solubility and dissolution rate, but rather it affects a number of pharmacological and technological aspects, as impurity profile, physico-chemical stability, manufacturability, and toxicity [43,44].

According to the IUPAC, a salt is a "chemical compound consisting of an assembly of cations and anions" [45]. Thus, a pharmaceutical salt is composed of an ionizable API (anionic, cationic, or zwitterionic) and a counterion that might be either molecular (*e.g.*, mesylate, acetate, …) or atomic (*e.g.*, bromide, sodium, …). Moreover, due to the requirement for charge balance, salts must have a definite stoichiometry [46]. Salts of acidic drugs have been commonly made using sodium (Na^+) as counterion, whereas for basic drugs chloride (from hydrochloric acid) is the preferred counterion. The reasons behind the choice of these two chemical species are merely based on accumulated experience [33]. In this context, Saal and Becker have provided an overview [43] on the usage of anionic and cationic salt formers, focusing also on maximum daily dosages for the most important administration routes (oral and intravenous). Another important class of salt formers is represented by L-α-aminoacids, which have become more and more important in the last years: it is today common to find lysine or arginine salts of an API, also for over-the-counter drugs. Their high water solubility makes them ideally suited for enhancing solubility properties of salifiable therapeutic compounds. An extensive review with many examples of aminoacids currently used as counterions in pharmaceutical preparation is available [22].

The solubility of the salt is governed by the solubility products of API and counter salt [33], and experiments revealed that salt formation affects the dissolution rate, rather than the solubility of the API itself. In particular, Serajuddin described some useful pH-solubility interrelationships of free acid or base forms and their salt, which helped to establish that the dissolution rate of a salt is usually faster than that of the API free form [41].

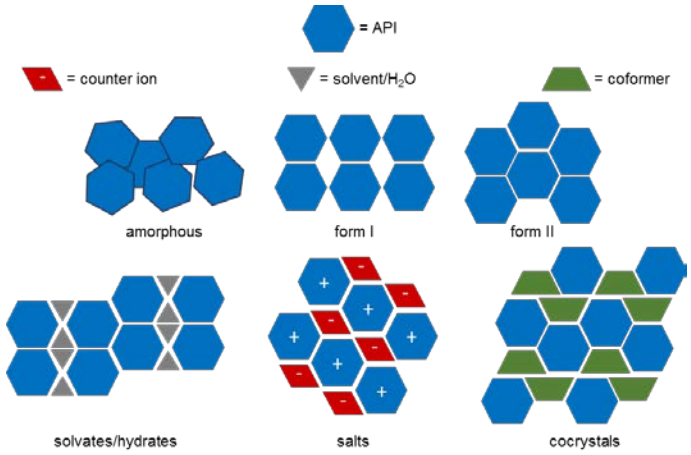

Fig. 1. Different possible solid-state pharmaceutical crystal forms for a generic API.

2.2 Cocrystals

The definition of cocrystal is subject to extensive debate at both chemical and legal level [40]. The most general definition states that "cocrystals are solids that are crystalline single phase materials composed of two or more different molecular and/or ionic compounds generally in a stoichiometric ratio" [39]. In this way, the definition comprises as cocrystals also compounds such as solvates, hydrates and certain metal complexes. These are however excluded using a narrower definition which simply adds to the previous one the following line "[…] which are neither solvates nor simple salts". Cocrystals are prepared from solid and neutral molecular substances at room temperature, yielding a homogeneous crystalline structure. If one of the two molecules (*i.e.*, coformers) is an API, a pharmaceutical cocrystal is formed. They are advantageous solid-state forms which improve the physicochemical properties of APIs, without changing the pharmacology of the drug, as its structure is not altered by intermolecular interactions.

The first cocrystal can be traced back to 1844 and Friedrich Wöhler, who grinded quinone along with hydroquinone [35]. He obtained the so-called quinhydrone, characterized by hydrogen bonding between the phenolic groups of hydroquinone and the ketonic ones of quinone.

Cocrystals represent a useful way of tuning properties of a given crystal, by choosing a suitable coformer that will form specific non-covalent bonds to yield an engineered supramolecular architecture. Therefore, this method makes it possible to modify the bioavailability of a drug by changing its dissolution rate, the thermal stability and hygroscopicity [47], which are necessary to preserve the product, the chemical stability (as in the case of cocrystals of explosives) [48], and also the mechanical properties [49]. Cocrystallization thus offers many opportunities; the possible applications of cocrystals make them of great interest to the scientific community and particularly among those involved in crystal engineering.

In the case of pharmaceutical cocrystals, coformers are substances defined as GRAS (Generally Recognized As Safe) by the FDA, *i.e.*, harmless compounds for human consumption [50].

From a certain point view, cocrystallization is similar to salification: a donor group of hydrogen bond gives rise to an interaction with an acceptor group. The main difference with salts is that cocrystallization does not cause a proton transfer between the two fragments involved. Hence, a salt and a cocrystal represent the two extremes of a continuum of supramolecular entities in which the proton transfer is more or less effective [51].

2.3 Ionic cocrystals (ICCs) and salt cocrystals (SCCs)

Two interesting subsets of cocrystals are ICCs and SCCs. ICCs feature an API and an inorganic alkaline or alkaline earth salt, for example NaCl or $CaCl_2$, in the same unit cell. SCCs encompass crystal forms wherein a salified API and a coformer (or *vice versa*) are in the same unit cell (Fig. 2).

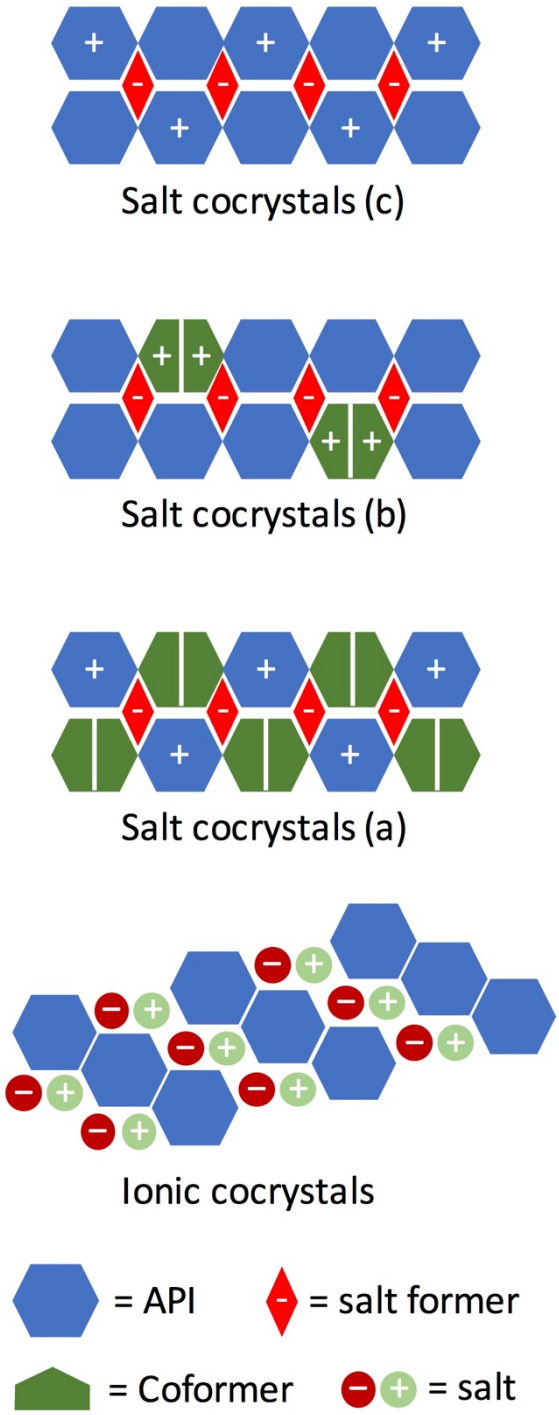

Fig. 2. Representative molecular arrangements of ionic cocrystals (ICCs) and salt cocrystals (SCCs). Depending on the type of SCC the unit cell is characterized by an API salt and a neutral coformer (a), a neutral API and coformer salt (b), and an API salt and a neutral API (c).

Analogous to cocrystals, the history of ICCs is a long one, covering at least 150 years [52]. Since the early reports, it was clear that these new crystal forms could be exploited to improve the dissolution behavior of APIs. The Braga's group has extensively explored ICCs, particularly focusing on their possible pharmaceutical applications: notable results concern the solubility properties of Barbituric acid and their modification by ICC formation with alkali bromides and with caesium iodide [12], the improvement of the physico-chemical properties of racetams and Nicotinamide with magnesium and calcium chloride [13,15], and the combination of lithium salts and Piracetam to yield ICCs which can be potential co-drugs, due to the synergistic effect of the lithium ion as medication and the nootropic Piracetam [14]. SCCs occur in several molecular arrangements, as depicted in Fig. 2: either the API (Fig. 2a and 2c) or the coformer (Fig. 2b) can be in a salt form, while the other component is neutral. The particular case wherein a SCC is composed of the API and its salt form (Fig. 2c) is of interest because of its characteristic of exhibiting two molecules of the same active principle in the same unit cell, without any extrinsic substance involved. As described by Brittain in 2013 [53], such a case typifies an attractive situation for pharmaceutical scientists since both coformers are basically the same chemical entity, thus they carry out the same pharmacological activity. An emblematic case is represented by Sodium Valproate-Valproic acid, a SSC approved by the US FDA and currently marketed under the brand name Depakote® [52,53]: salt-cocrystallization has allowed to maintain the pharmacological function and manufacturability of sodium valproate while ruling out its high hygroscopicity. Hence, improved stability over time was achieved [54].

Our group has exploited SSCs to enhance the dissolution and thermal stability properties of two APIs, namely Niclosamide and Tolfenamic acid [10,11]; results from other authors confirmed that SCCs are in general a valuable alternative to tailor the pharmacological properties of drugs [9,55].

3. Design & synthesis techniques

The design and preparation of salts and cocrystals is a multi-stage process, often empiric. Some decision models have been proposed in the literature with the purpose of rationalizing the process [56–60]: each model comprises a series of sequential decisions (a tree) aimed at maximizing the solubility, or determining the most appropriate experiments for the drug candidate. For example, Tong et al. [58] proposed a multi-tier approach to salt selection for poorly soluble compounds. The salt screening is performed in the first step; in the other steps, in vitro and in vivo studies (on animals) are carried out. The final tiers are physico-chemical and manufacturability assessments.

Salt screening is an early part of drug development, and is crucial for selecting the optimized form(s) of an ionizable API that will be taken forward to the next stages of the process. Salt formation is an acid-base reaction which depends primarily on the pK_a difference between the acid and the base; therefore, the experimenter needs to screen numerous salt-forming agents by choosing among those that give a pK_a difference equal to or greater than two units with respect to the drug. Other than pK_a, additional parameters should be considered when salt screening is performed, such as solvents, crystallization conditions, techniques, solubility, chemical stability, and toxicity [44,57]. The large parameter space and the repetitiveness of the experimental procedure make the salt screening suitable for automated systems: thus, automatic high-throughput screening (HTS) techniques are available for the task, especially when rapid salt selection is required [61]. Some limitations do, however, exist for HTS, including small sample quantity, which may lead to reproducibility issues when performing scale-ups, and large amount of data to be analyzed. Hence,

manual salt screening techniques are still of importance, and several efforts have been made in the literature to assess the best approach: Collman et al. have compared a rational salt screening approach to the HTS approach [44]. An example of rational approach, which is reported in Fig. 3, requires fewer trials than HTS, common laboratory equipment, and reduces the difficulties of scaling up the reaction, since it mimics the techniques used by process chemists. The results of the study indicated the superiority of the rational screening approach to the HTS. Simplicity, flexibility, and a relatively higher reliability than HTS have been identified as the key factors responsible for this outcome.

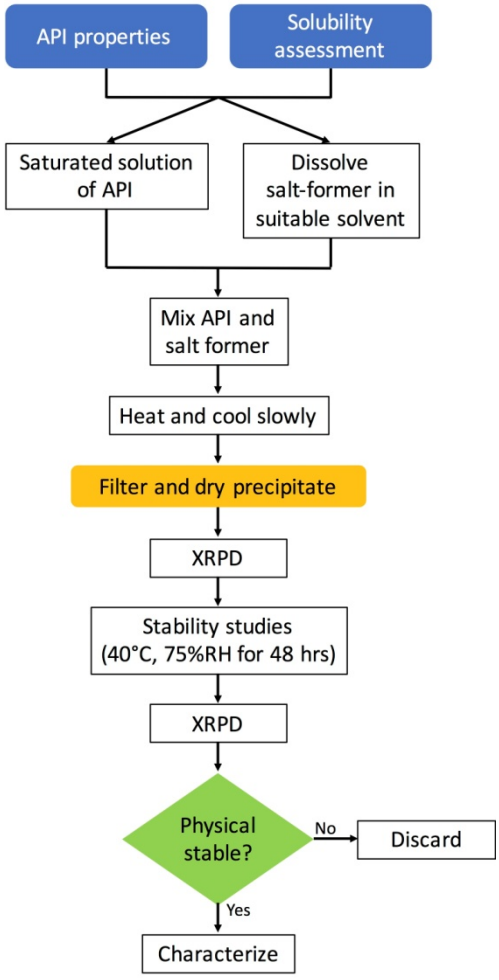

Fig. 3. Outline of the rational salt screening approach as performed by Fernández Casares et. al. (see ref. [62]). Reproduced with permission from ref. [62], Copyright 2015 Royal Pharmaceutical Society.

Fernández Casares et al. have recently compared [62] three different salt screening methods, namely in-situ, rational salt screening, and HT. They concluded that the rational salt screening is the preferred approach on the basis of efficiency, quick turnaround time and information generated. The authors, however, pointed out that the results are strongly influenced by the solubility of the API, independently from which method is chosen.

Similarly to salts, design strategies of pharmaceutical cocrystals have also been developed, and several thorough reviews exist [8,63,64]. Preparation of cocrystals is clearly an aspect of chemical

synthesis, thus it displays the same characteristics [40]. As such, the synthesis of new crystalline forms is affected by many variables which are related primarily to the nature of the solvent and the reactants. For example, one must carefully evaluate the presence of competing functional groups, the solubility of reactants in the solvent, as well as a plethora of experimental conditions, namely stoichiometric ratio, temperature, stirring, pH, and the type of glassware, to name but a few.

In this regard, some techniques revealed to be advantageous for maximizing the probability of successful outcome in supramolecular synthesis, thus they are commonly applied: neat grinding, kneading (also known as liquid-assisted or solvent-drop grinding), slurrying, co-melting, vapour digestion and all type of co-crystallizations from solvent (from slow evaporation to crystallization at interfaces or with antisolvents) are usually indicated for both screening and production of cocrystals. However, as pointed out by Braga and coworkers [34] there is still a lack of control over nucleation, crystallization, and composition of the crystalline phases; this ultimately represents the major drawback of cocrystal synthesis, besides being a considerable scientific challenge.

More exotic approaches such as sonication [65], sublimation [66], vapour digestion, supercritical carbon dioxide [67], and spray drying [68] are usually applied when other screening techniques fail, or when searching for higher yields.

A few studies have addressed the problems of cocrystal synthesis [69–72]; as a general conclusion, mechanochemical methods appear to be superior to solution methods, although more proof is definitely needed to solve the issue. Accordingly, mechanochemical approaches have received substantial attention over recent times, because they offer a greener and affordable synthetic pathway to supramolecular structures [73]. The process can be carried out either

r in a mortar (usually agate), or in a ball mill. Usually, trials are performed in either dry or wet conditions (also called liquid-assisted or solvent-drop grinding, or kneading): the latter requires the addition of catalytic amounts of solvent, with the double advantage of facilitating cocrystallization kinetics towards higher degree of crystallinity, and to allow a greater control over the formation of polymorphs [72,73]. These methods present however several disadvantages: first of all, the product is in the form of a microcrystalline powder, thus a subsequent campaign of experiments has to be performed for obtaining single crystals for crystal structure characterization. The mechanical energy generated during ball milling or kneading has indeed the effect of increasing the crystalline disorder, and the so obtained products have thus a lower degree of crystallinity than the ones from solution methods [74]. Secondly, the scale-up of mechanochemistry to industrial production presents clear implementation difficulties, which are not expected to be overcome in the near future.

There are two main theoretical models seeking to explain the mechanisms of mechanochemical reactions. The first is the so-called “hot spot theory”: the frictional processes which set in due to the lateral friction of particle surfaces determine a local temperature increase at the contact points up to 1000°C for short periods of the order of ms. The second is the magma-plasma model, which considers impacts, rather than frictional forces, between particles, that give rise to transient plasmas responsible for temperatures of the order of 10,000°C which in turn activate the reaction [73].

These models do not however explain how molecules can withstand such extremely high temperatures without breaking down into atoms and ions. Actually, these theories were delineated for inorganic compounds, whereas the cocrystallization of organic solids needs other hypotheses. In this regard, three processes were proposed to account for organic cocrystals formation: the first one considers the mobility of molecules in solids, which makes them capable of moving through the surface or the bulk of the crystal. In contrast, for molecules exhibiting dense patterns of hydrogen bonds in their crystal structures, hence less likely to show a high degree of mobility, the possibility

of the temporary formation of amorphous phases has been proposed. Lastly, microscopic observations found evidence of the formation of a eutectic intermediate, which subsequently nucleates to form the solid cocrystals [75]. The cocrystal phase that originates at the interface between the surfaces of the two reactants is separated gradually following its formation, to give a nearly quantitative yield of reaction (Fig. 4).

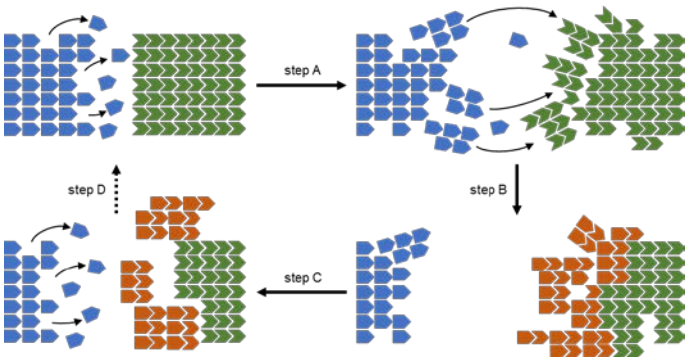

Fig. 4. Proposed mechanism for the formation of cocrystals by mechanochemical grinding. Step A: Mechanochemical activation of the reactants' surfaces; step B: mechanochemical removal of the cocrystal from the surface; step C: cocrystal formation and nucleation; step D: process continues. Adapted with permission from ref. [75]. Copyright (2009) American Chemical Society.

Although still based upon a trial-and-error approach, mechanochemistry is regarded as a possible mainstream supramolecular synthesis technique of the future. On the other hand, Aakeröy has very recently remarked [40] the importance of doing more research in the field, to develop more robust and versatile cocrystallization strategies.

4. Characterization challenges and techniques

Crystallography, including powder and single-crystal XRD (PXRD and SCXRD, respectively), spectroscopy (vibrational and magnetic), microscopy, thermal analysis (differential thermal analysis, DTA; differential scanning calorimetry, DSC; thermogravimetric analysis, TGA) and other physical techniques are the primary techniques used, alone or in combination with one another, to characterize novel forms and to examine functions of salts and cocrystals in the solid state.

SCXRD, in particular, has become a cornerstone of most crystal form research programs since the structural information derived is unparalleled. In many cases, it allowed to validate crystal engineering strategies based on preferred hydrogen bonding motifs. In the same time, it often revealed the unpredictable nature of molecular self-assembly. Furthermore, X-ray structures permit a variety of solid-state properties, such as morphology, hygroscopicity, porosity, stability, compressibility, and so on to be modeled and/or predicted and related structures to be engineered.

SCXRD confirms composition, packing and hydrogen bond arrangements but single crystals are not necessarily always available from the discovery stage. Indeed, often, the structures of small molecules are elusive either because size or quality of the crystals do not fit the requirements of the XRD methods or because the synthetic methods (e.g. mechanochemistry or solid-state methods) lead to amorphous or microcrystalline powders. In the last decade, increasing attention has been given to new synthetic routes besides traditional crystallization from solution (see above Section 3).

Remarkable results have been obtained by solvent-free methods such as grinding and kneading [73,76], co-melting [77], and also by dehydration/desolvation of hydrated/solvate crystal forms leading to crystal cracking [78]. However, as already pointed out, with respect to crystallization from solution, these less conventional methods generally produce polycrystalline powder materials, for which structural determination is (relatively) less straightforward. Polycrystalline samples can be used to seed crystallization processes in order to grow single crystals amenable to XRD [79–81]. If the seeding procedure is unsuccessful or not practicable, the structure of the new form can be determined via PXRD [82,83]. For example, Lapidus et al. [84] determined crystal structures of 10 cocrystals from high-resolution synchrotron PXRD. Direct space (for example, simulated annealing [85] parallel tempering [86], evolutionary algorithms and other global optimization algorithms) [87], reciprocal space (such as direct and Patterson methods) [88] and dual-space (charge flipping [89] and other hybrid approaches) methods, provided in several user friendly software programs, allow for crystal structure solution from powder diffraction data even with conventional sources. However, crystal structure determination from powder is still characterized by lower success rates compared to SCXRD. Furthermore, while SC- and PXRD provide the same intrinsic information, when three-dimensional data is compressed into a one-dimensional powder pattern, information is lost (obscured by peak overlap) and the loss of symmetry independent reflections in a one-dimensional powder pattern decreases both confidence level and accuracy. In principle, these quality factors can be improved if complementary information obtained from other sources, i.e. advanced spectroscopic techniques, is supplied. For example SSNMR can provide essential information, such as the number of independent molecules in the unit cell (Z'), the presence of disorder, hydrogen bonding properties, salt or cocrystal character, as well as the presence of either water or solvent molecules [90–93], which help in finding reliable starting structures and improving the quality and speed of the crystal structure determination process, from the initial indexing stage to the final Rietveld structural refinement. As an example, the structure of the salt Lidocainium hydrogen succinate was determined from laboratory PXRD pattern assisted by SSNMR data (Fig. 5 and Fig. 6) [94]. Advanced 2D SSNMR techniques (^{1}H DQ CRAMPS and ^{1}H–^{13}C long range HETCOR spectra) provided useful insights on ionic character of the adduct, number of independent molecules, crystal packing and hydrogen bond environments through the analysis of $^{1}H-{}^{1}H$ or $^{1}H-{}^{13}C$ proximities [95,96].

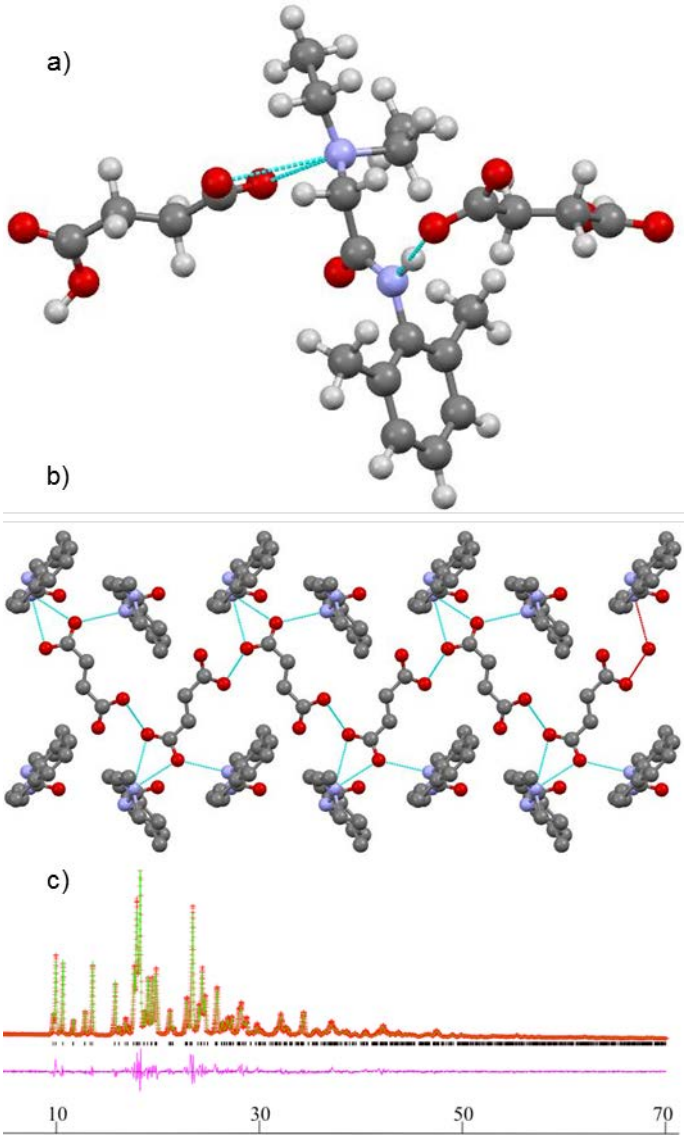

Fig. 5. PXRD structure of the Lidocainium hydrogen succinate salt. a) Relevant hydrogen bonding interactions between the Lidocainium ion and the hydrogen succinate. b) Hydrogen bonding patterns. H atoms not shown for clarity. c) Experimental (red crosses), calculated (green) and difference (purple) patterns for crystalline Lidocainium hydrogen succinate. Adapted with permission from ref [94]. Copyright (2013) American Chemical Society.

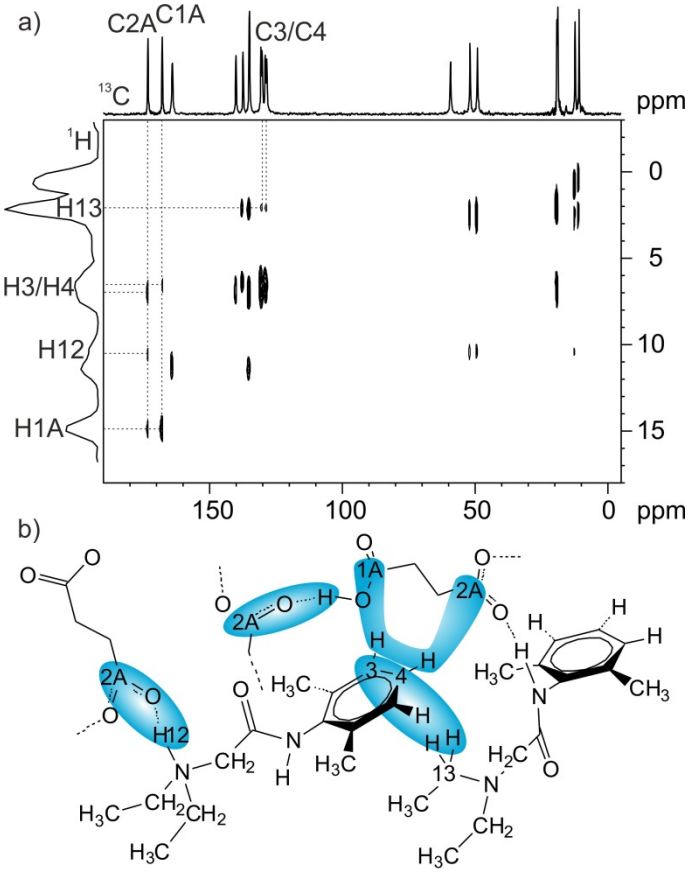

Fig. 6. (a) ^{1}H-^{13}C (400 and 100 MHz) FSLG off-resonance HETCOR spectra of the Lidocainium hydrogen succinate salt with main long-range ^{1}H-^{13}C correlation. (b) Representation of the crystal structure showing the main ^{1}H-^{13}C intermolecular proximities useful for speed and improve the PXRD structure solution. Adapted with permission from ref. [94]. Copyright (2013) American Chemical Society.

Vogt et al. [97] demonstrated that SSNMR can be effective for the characterization of cocrystals by diagnosing hydrogen bonding and local conformational changes through ^{1}H–^{1}H, ^{1}H–^{13}C and ^{19}F–^{13}C coupling. Maruyoshi et al. [98] identified COOH···N_{arom} and CH_{arom}···O=C interactions in an Indomethacin·Nicotinamide adduct by using 2D ^{1}H DQ and ^{14}N–^{1}H and ^{1}H–^{13}C heteronuclear magic angle spinning (MAS).

In a similar way, the sensitivity of mid-IR and Raman spectra to the solid-state forms has rendered them equally useful in supporting PXRD data for chemical structure identification based on functional groups, phase identification, for in situ analysis of time-dependent crystallization, for cocrystal screening [99] and for hydrogen bonding analysis based on characteristic bond stretching and bending frequencies. Indeed, vibrational spectroscopies provide definitive fingerprints of molecules either directly by their absorption of IR or mid-IR radiation over the range of 4000–400 cm^{-1} or through inelastic scattering of radiation which produces Raman shifts from the excitation laser wavelength over the range of 3500–50 cm^{-1}. Desiraju identified molecular cocrystals sustained by amide dimers from diagnostic N–H···O bands in their IR spectra [100] Raman spectroscopy has been used to study cocrystals, including their formation during high-throughput slurry screening and to distinguish between homogeneous (cocrystals) and heterogeneous mixtures in formulated tablets [99,101].

Thermal analyses such as DTA, DSC and TGA provide information on melting, crystallization, sublimation, decomposition and solid-state transitions, and also enable the observation and quantification of volatile components (residual solvent or gaseous by-products). This wealth of data is useful to establish manufacturing and storage conditions, and to characterize both solvates and hydrates [102].

Also optical (light) microscopy, in particular with microscopes equipped with a circular rotatable stage and two polarizers, can provide useful information. Indeed, each molecule produces crystals with different and peculiar optical properties. Although electron and atomic force microscopies, which operate at considerably higher magnifications, have to a large extent superseded optical microscopy for chemical analysis, light microscopy can still yield a wealth of information on the crystal structure and composition of materials, salts and cocrystals included. Thermomicroscope or hot stage microscope (HSM), a microscope coupled with a hot-stage accessory (either open or closed), provides an invaluable wealth of information for physical characterization of pharmaceutical materials [103]. It combines the best properties of microscopy and thermal analysis to enable the solid-state characterization of materials as a function of temperature [104]. It allows either to identify localized thermal inhomogeneities on the sample surface missed by DSC but captured in the HSM images. It also enables to obtain visual and semi-quantitative information on polymorphic transitions and thermal behaviour displayed by different crystal forms of drugs [105,106] and to identify the formation of new solid phases or even drug-drug and drug-excipient interactions.

X-ray photoelectron spectroscopy (XPS), a surface technique for chemical analysis, can be useful in the crystal form structural characterization since, like SSNMR spectroscopy, it is sensitive to changes in the chemical environment of individual atoms. It probes the amount of energy required to emit an electron from an atomic core level. Interestingly this amount of energies is often fundamental to directly measure proton transfer in the solid state. Indeed, XPS was applied to differentiate between a salt and a cocrystal [107].

Terahertz time-domain-spectroscopy (THz-TDS) is a vibrational spectroscopic technique that probes the IR active vibrational modes in the far-IR and sub-millimeter region. It has emerged as a versatile spectroscopic technique and an alternative to PXRD in the characterization of molecular crystals. It interacts with those vibrational modes directly related to the crystal packing which represent vibrations of the whole molecule rather than just of single functional group within molecules, as is the case in IR-spectroscopy. It is also suitable to probe noncovalent interactions, such as hydrogen bonds and related supramolecular synthons reflecting variations in the intermolecular interaction networks between different crystal structures. THz-TDS has been used to distinguish between chiral and racemic molecular cocrystals of malic acid and tartaric acid with Theophylline [108].

SCXRD remains the technique of choice for accurately locating atomic positions, as well as measuring anisotropic displacement parameters, in crystal structures; however, Fourier difference maps derived from XRD often give an ambiguous answer concerning hydrogen atom positions. However, hydrogen bond as well as hydrogen bonded structures naturally involve hydrogen atoms. This represents a remarkable limitation since the hydrogen bond is the interaction of choice in the making of crystal forms, because it combines strength, directionality, and, at least to a considerable extent, predictability. X-rays are scattered by the diffuse electrons of an atom. Since the scattering intensity varies monotonically with Z, the scattering power of the single electron of a hydrogen atom is very low. Furthermore, it is typically displaced towards the atom that it is bonded to. The

problem can be overcome by neutron diffraction which precisely locates hydrogen atoms and unequivocally characterizes proton transfer in the solid state. Indeed, neutrons are scattered by the nuclei rather than electron density. This difference is especially significant for hydrogen atoms, because not only is the neutron scattering power of H comparable to that of C, O and N but the center of gravity of the neutron also perfectly defines the atomic position [109–111]. In this way, neutron diffraction has been used to provide highly accurate structural details associated with hydrogen atom positions in crystals. However, it is not routinely accessible. Thus, nowadays, one of the fundamental challenges that scientists and pharmaceutical companies have to face in the structure characterization concerns the position of the hydrogen atoms along hydrogen bond interactions. Whether the achieved crystal forms ought to be regarded as neutral molecular cocrystals or as ionic molecular salts in many cases remains an unanswered question. Indeed, all hydrogen bonds were likened to an incipient proton transfer reaction, which, of course, is the key reaction transforming what might otherwise be a cocrystal into a salt. However, it is not always possible to predict the outcome of the reaction. The difference is subtle depending on whether the proton along a D − H···A contact remains close to the donor acidic group (D) or moves close to the basic acceptor (A) or will adopt some intermediate location along the D···H···A vector. There are several examples in the literature [112] where the position of the proton is shown to move along the D···H···A axis [51,113]. Proton transfer from the acid (donor) to the base (acceptor), besides depending on the relative values of pK_a (but beware of the fact that pK_a is evaluated with respect to the solvent, usually water, and not in the solid state) [26] also depends on the temperature as well demonstrated for a pentachlorophenol:pyridine 1:1 complex, as well as for the ternary 4-dimethylaminobenzoic acid:3,5-dinitrobenzoic acid:4,4’-bipyridine complex recently reported by Thomas et al. [114]. Still in 2014 [115], crystals of an API-coformer complex were defined as a salt or cocrystal exclusively based on ΔpK_a ($pK_{a(base)}$—$pK_{a(acid)}$), without any experimental evidence, with complexes defined as “salts” if ΔpK_a was at least 1 and “cocrystals” if ΔpK_a was less than 1.

It is important to recognize that the terms ‘salt’ and ‘cocrystal’ are not meant to be mutually exclusive, except perhaps for simple acid–base pairs, where the only distinguishing feature of a salt and a cocrystal is the location of the acidic proton in the crystal structure.

Although the distinction between salts and cocrystals seems to be relegated to academic concerns about the position of the H atom along the hydrogen bond axes, it deeply involves also companies, regulatory bodies and final physical properties. Indeed, it can be significant from a regulatory and intellectual property perspective since regulatory bodies such as the FDA treat both types of multicomponent crystals differently [116]. Thus, this information is essential to related parties who use specific API as a compound of interest. Today, regulatory path for new salts requires more testing and clinical data when submitted to the U.S. FDA as a 505(b)(2) Abbreviated New Drug Application (ANDA). On the other hand, testing requirements for the generic market entry of cocrystals have not been established [117]. Because of the potentially different regulatory pathways that may arise for salts and cocrystals in the future, it is fundamental to keep in mind which techniques specifically enable to probe ionization in the solid state. It is also true that all salts and cocrystals are potentially useful from a final physical property and intellectual property perspective. Aakeröy et al. have noted dramatically different structural behavior between carboxylic acid cocrystals and carboxylate salts [27]. Often, salts may be more desirable because the intrinsic solubility of a salt in water can be higher than a cocrystal: indeed a cocrystal with a negative pK_a, once dissolved, yields the non-ionized API whereas a salt will yield a generally more water soluble

ionized API. However, when the dissolution rate is more important than the equilibrium solubility, a cocrystal can be more advantageous than a salt form. For instance, it has been demonstrated how a rapidly dissolving cocrystal of an API with low water solubility significantly increased the bioavailability of the API [118]. Also, the melting behavior is particularly important when selecting a salt or cocrystal for a drug product, since processing steps, such as milling or micronization, can generate considerable heat which not all salt and cocrystal forms are equally able to tolerate.
However, in which way the location of the proton affects the physical properties relevant to the stability or to delivering a drug in a controlled manner or to determine manufacturing properties is in many cases unclear. The debate over whether salts or cocrystals will display more useful physical properties is in any case API and project specific.
That said, from the characterization point of view, the intrinsic limitations of XRD techniques in detecting the hydrogen atom positions prompted scientists to explore and developed spectroscopic tools to solve this issue. Single crystal neutron diffraction, SCXRD, SSNMR analysis, vibrational spectroscopy, XPS are the techniques either alone or combined with each other that most of all provide reliable evidences about the position of hydrogen atoms. Among these methods, an emerging approach that deserves mention is that of Density Functional Theory (DFT) calculations used either to support the SSNMR data or even alone carried out to obtain an optimized structure of both neutral and anionic forms of a certain drug.

4.1 Single crystal X-Ray Diffraction

Close inspection of SCXRD structural parameters, such as bond lengths and angles, can also reveal whether or not ionization has occurred. The use of low temperature and copper radiation to obtain more accurate bond lengths is generally recommended. When the cocrystal displays carboxylic groups involved in hydrogen bonding, the decision about the nature of the complex depends on the C-O distances. The C–O bond lengths in carboxylate salts have been shown to be within 0.03 Å of one another, while neutral carboxylic acid C–O bond lengths may differ by more than 0.08 Å (1.2 Å for C=O, 1.3 Å for C–OH) [114,115]. However, the C-O bond distances can only assist in the distinction between a salt or a cocrystal when carboxylic acids are utilized as a crystallization agent [51,121]. In addition to C-O bond lengths and angles, also a careful inspection of intermolecular contacts and torsion angles can indirectly reveal the ionization state of an acid or base in a crystal structure. This is the case of the 2:1 complex between a Gemcitabine prodrug and the p-toluenesulfonic acid. The ionic character of the cytosine rings in the Gemcitabine prodrug was ascertained through a Cambridge Structural Database survey by checking in other similar ionic structures the compatibility of the measured bond distances and angles with proton transfer.

4.2 Vibrational spectroscopies: IR and Raman

While deprotonation of a carboxylic acid to form a salt is not only expected to perfectly equalize the C–O bond lengths, it has also been shown to have a dramatic effect on the C=O/C–O stretching vibrations observed by IR/Raman spectroscopies. These techniques provide faster and simpler analysis when compared to XRD and use small amount of powder and do not require long-range order nor large single crystals. Whereas a typical carboxylate anion gives rise to two carbonyl stretching bands, a strong asymmetrical band below 1600 $cm^{-1}$and a weaker symmetrical band near 1400 cm^{-1} [122] neutral carboxylic acids in cocrystals have strong C=O absorption bands above 1600 cm^{-1} (near 1700 cm^{-1}), along with weak C–O absorption bands near 1275 cm^{-1} that confirm un-ionized states of the adduct. Mukherjee et al. and Chakraborty and co-workers performed

vibrational spectroscopy experiments to identify the hydrogen bond pattern present in multicomponent molecular crystal structures [100,123]. There are reports of IR spectroscopy used to evaluate if the proton transfer has occurred or not between the pharmaceutical ingredient and the counterion, in salt phases, or between coformers in cocrystals, respectively [51,123–125].

Similarly, Raman spectra of binary mixtures of Indomethacin and several coformers after 7-day slurried were compared with the spectra of γ- and α-Indomethacin and of the 1,4-dioxane solvate in the shift region 1635–1715cm^{-1} attributable to the stretching of C=O bond. The Raman spectra indicated that Indomethacin could structure neutral cocrystals with D/L-mandelic acid (IMC–MDA), Nicotinamide (IMC–NTA), lactamide (IMC–LCA), benzamide (IMC–BZA) and saccharin (IMC–SAC) and form ionic salts with Tromethamine and N-methyl-D-glucamine [99].

In a recent paper, J. Lu and coworkers [126] analyzed vibrational spectroscopic data of cocrystals of Sulfamethazine (STH) and Sulfamerazine (SMZ) with p-aminobenzoic acid (PABA) obtained with different mechanical methods including neat cogrinding and solvent-drop cogrinding. The Raman spectra of pure STH has bands at 1342 cm^{-1} and 1637 cm^{-1}, corresponding to N–H deformation and NH_2 bending, respectively. Such bands are shifted to 1359 cm^{-1} and 1627 cm^{-1} in the cocrystallization product of sulphametazine with PABA obtained by solvent-drop cogrinding. Slight band shifts are a clear indication that a cocrystal was formed, since a shift of 30 to 40 cm^{-1} are expected in the case of a salt [127]. The increase in the in-plane N– H deformation frequency of STH from 1342 cm^{-1} to 1359 cm^{-1} indicates that the sulfa N–H (linked to sulfonyl) is participating in the hydrogen bonding. Interestingly, PABA and SMZ with a ΔpK_a of 2.13 form a binary eutectic, while PABA and STH with a larger ΔpK_a of 2.59 can form a cocrystal in the ratio of 1:1. This is a clear indication that not only the ΔpK_a but other parameters such as as stereo-hindrance effect, intramolecular hydrogen bonding, etc. should be taken into account during the design of pharmaceutical cocrystals.

4.3 Solid-state Nuclear Magnetic Resonance

Among all characterization techniques, SSNMR is unparalleled with respect to the diversity of techniques designed specifically to probe structure and dynamics with site selectivity, not to mention examine phase/component miscibility. One of the important aspects of this nondestructive technique, besides its high complementarity with XRD, is the multinuclear approach. Owing to its ability to probe either carbon, nitrogen or even directly the hydrogen atoms it gives information on several types of contacts according to strength and geometry for structural elucidation [95,128]. Strong (single well and low barrier), moderate and weak hydrogen bonds have been easily detected and characterized [129] but most of all the position of the hydrogen atom is easily established through a wealth of parameters.

The main SSNMR parameters that can provide insights on the ionic or neutral nature of the crystal forms in the solid state are (a) the chemical shift, (b) the dipolar interaction, (c) the chemical shift anisotropy (CSA), (d) the relaxation times (T_1 and T_2) and (e) the isotopic effect. All these parameters can be obtained and evaluated for each NMR active nucleus involved in the weak contact, be it ^{1}H, ^{19}F, ^{13}C or ^{15}N over a wide timescale without the requirement for long range order or even homogeneous samples [130]. The influence of hydrogen bonds on these nuclei has been recently reviewed [131]. ^{1}H, ^{13}C and ^{15}N SSNMR chemical shift data can be used to detect and to estimate the presence and the strength of hydrogen bonds as well as the occurrence of proton transfer from the acid to the base with formation of charge-assisted contacts. Thus, not only is

SSNMR spectroscopy well suited for identifying polymorphs and solvates in bulk APIs, but it can also provide detailed structural information from dipolar based pulse sequences [132] useful for both confirming structure solutions obtained by powder diffraction and rationalizing materials in terms of molecular or ionic crystal structures [95].

4.3.1 ^{1}H chemical shift

The development of line narrowing techniques in solids i.e. the possibility of spinning the sample at MAS speeds up to 110-120 kHz, allows the location of chemical shifts of hydrogen-bonded protons leading to an increasing number of ^{1}H studies [133]. Applications of the latest developed high-resolution ^{1}H SSNMR technologies and techniques have been recently reviewed [134].

In particular, the proton is increasingly deshielded with increasing the hydrogen bond strength, which leads to 1H high-frequency shifts far from the aliphatic and aromatic signals (Scheme 3). However, the magnitude of the shift is directly correlated with the length of the hydrogen bond [109,131] rather than with the neutral or ionic character of the interaction.

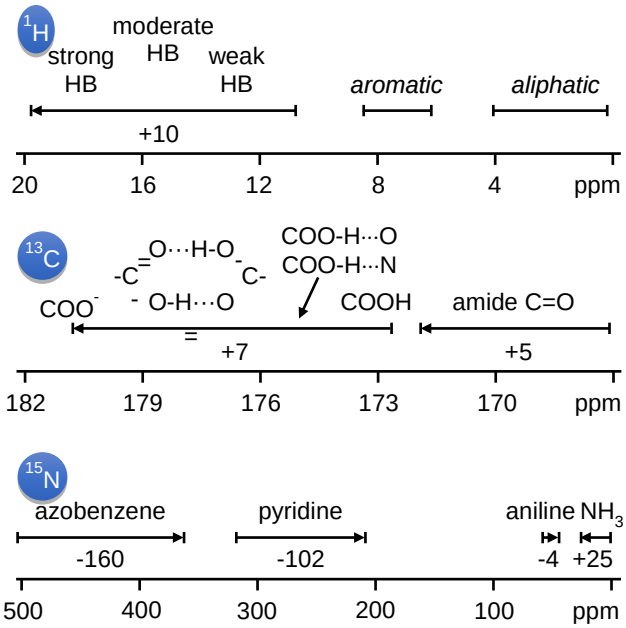

Scheme 3. ^{1}H, ^{13}C (limited to carboxylic and amide carbonyl groups) and ^{15}N SSNMR shifts due to hydrogen bond formation and proton transfer occurrence.

4.3.2 ^{13}C chemical shift

On the other hand, ^{13}C and ^{15}N chemical shifts better reveal the formation of cocrystals or salts in particular when carboxylic or nitrogen-containing functional groups are present in the API or in the co-former. Their values are correlated to presence of hydrogen bonds and proton position along the interaction axes accordingly to functional group, whether carboxylic or carbonyl for ^{13}C and aliphatic or aromatic for ^{15}N (Scheme 4).

The ^{13}C SSNMR is a commonly used method for identifying the existence of proton transfer. It is well-known that a change in the chemical bond such as proton transfer can change the respective spectra, as well. In the case of ^{13}C signals of carboxylic groups, the shift upon hydrogen bond formation is of about 3-7 ppm always toward higher frequencies and linearly increase with decreasing N···O distances. If a proton transfer occurs across the hydrogen bond, with formation of a carboxylate group and a charge-assisted N^{+}-H···O^{-} contact, the high-frequency shift is maximum

(around 6-7 ppm) [135]. However, one has to be aware of very strong hydrogen bond, such as those formed in the cyclic dimerization of the COOH functions, which usually present chemical shifts similar to that of carboxylate groups (~2 ppm lower) [136,137].
The protonation state of Ibuprofen in five tablets produced by different manufacturers has been evaluated by comparing their ^{13}C cross-polarization magic-angle spinning (CPMAS) spectra and SEM images with those of the pure Ibuprofen and its sodium salt [138]. The COOH carbon of pure Ibuprofen falls at 183.1 ppm while the COO^- in the sodium salt gives rise to two signals at 184.0 and 184.9 ppm, for the two independent molecules. The analysis of the Ibuprofen COOH signal in the tablets' spectra confirms that the API is in a protonated state in all investigated tablets. These results find support on chemical shifts calculated based on DFT methods. The small difference in ppm observed for the carboxylic signals between the neutral and ionic forms is attributed to the presence of the cyclic dimerization of the COOH functions in the structure of pure Ibuprofen which shift the COOH chemical shift at high frequencies.
The ionic nature of the adduct between fumaric acid and Lamivudine (β-L-2',3'-dideoxy-3'-thiacytidine, 3TC), a nucleoside-based anti-HIV/HBV drug that has provided insights into the nucleic acid double-stranded helix assembly, has been ascertained through the ^{13}C shift of the fumaric acid carboxylic signal at 176.3 ppm corresponding to a carboxylate group [139]. ^{15}N SSNMR spectra confirm the protonation of the nitrogen atoms with a shift from 201.2 for the free base form II to 143.3 ppm in the salt.
Even if not directly involved in the proton transfer, shifts in the signals of carbon atoms may also be diagnostic of the salification of the nitrogen atoms which are directly bonded to. An interesting case is represented by Dimenhydrinate (DIM), an important drug used for the prevention of motion sickness, which is known as a multicomponent crystal consisting of two drugs: Diphenhydramine (2-benzhydryloxy-N,N-dimethyl-ethanamine) and 8-Chlorotheophylline (8-chloro-1,3-dimethyl-7H-purine-2,6-dione) [140]. By comparing the experimental and calculated spectra, it has been possible to determine the presence of proton transfer on the nitrogen atom. The large shift (around 7 ppm) observed for the carbon atom C18 (that bonded to the N^+) supports the data validity regarding proton transfer. The slight shifts in the other carbon atoms (C15, C16, C17, and C19) also strengthen the presence of proton transfer since these atoms surround the protonation-deprotonation site in 8-Chlorotheophylline and Diphenhydramine molecules.

4.3.3 ^{1}H and ^{13}C chemical shift anisotropy

Owing to tensorial nature of the chemical shift, its isotropic value (δ_{iso}) represents an average of three components, the chemical shift tensors δ_{11}, δ_{22} and δ_{33}. Knowledge of the chemical shift tensor values and their orientations with respect to a molecular axis system has at least two important consequences: a) they can be correlated with geometry of the chemical bond, i.e. with the structure of a molecular fragment, since they are strictly related to the distribution of electron density around nuclei; b) more important for application of SSNMR, their values and orientation for some functional groups are rather conservative parameters and can be fixed relative to a molecular reference frame for a small fragment. This suggests that variations in individual principal components might be more sensitive indicators of the proton transfer reaction across a hydrogen bond interaction i.e. of protonation state of a carboxylic group, than the isotropic chemical shift alone [141–145].
It is worth noting that the chemical shift tensors can be obtained for every nucleus involved in a hydrogen bond interaction: ^{1}H, ^{13}C, ^{15}N or even ^{17}O. However, measurements of the ^{1}H shift tensors

in solids are challenging because of strong ^{1}H homonuclear dipolar couplings and the relatively small size of the ^{1}H CSA interaction. Some progress has now been made towards general and robust recoupling methodologies based on two-dimensional NMR experiments which correlate the anisotropic and isotropic parts of the interaction [146–152]. However, while proton CSA has been successfully correlated to inter/intramolecular hydrogen bond features (O-H distances or O-H···O angle) [147–149] no papers have been devoted to correlate their variation as a function of charge-assisted or neutral interaction i.e. salt or cocrystal formation.

In a similar way, also ^{13}C chemical shift tensor values and orientation provide insights on strength and geometry of the hydrogen bond interaction and change significantly with the protonation state of the carboxylic groups. Differently to ^{1}H, they can be easily obtained on a single crystal by static NMR measurements [91] or by analysis of spinning sideband manifolds in low spinning speed spectra [156,157]. Several procedures have been developed for recovering CSA information on fast-spinning MAS NMR experiments without sacrificing sensitivity and resolution [158,159]. When the number of peaks leads to a strong spinning sideband overlap, the 2D PASS (Phase Adjustment Spinning Sideband) technique is the preferred choice since it can separate the isotropic chemical shift in the direct dimension from the anisotropic pattern associated at each distinct site in the indirect dimension [155,156]. The orientation of the three CSA tensors for a generic carboxylic group COOH is depicted in Scheme 4.

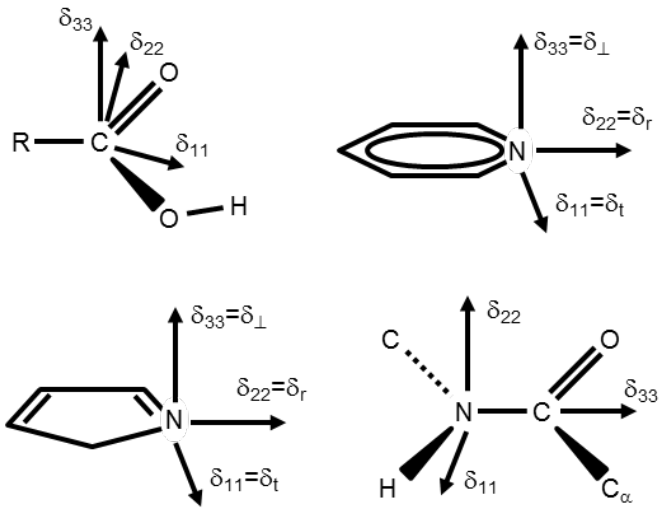

Scheme 4. Orientation of ^{13}C and ^{15}N chemical shift tensors (δ_{11}, δ_{22} and δ_{33}) in (a) carboxylic groups (^{13}C), (b) pyridine (^{15}N), (c) pyrrole/pyrazole/imidazole derivatives (^{15}N) and (d) amide groups (^{15}N).

δ_{11} lies in the plane of symmetry of the carboxylic group and it is directed along the R–C axis in the deprotonated form and perpendicularly to the C=O group in the protonated case, δ_{22} lies perpendicular to the plane of symmetry of the C=O and it is the most diagnostic parameter reflecting the protonation state of the group. δ_{33}, the most shielded tensor, is perpendicular to the plane of symmetry.

Studies of protonated and deprotonated carboxylic group in amino acids have shown that the values of the principal elements of the nuclear shielding tensor change significantly upon hydrogen bond formation and with the protonation state of the carboxylic groups [142,162]. In a similar way, it has been demonstrated for aliphatic dicarboxylic acids that δ_{11} values change from 242±2 ppm

(carboxylate form) to 257±4 ppm (carboxylic form), δ_{22} values are of 177±10 ppm for the COO^- group and 155±20 ppm for the COOH moiety representing the most sensitive parameter to the localization of the hydrogen atom [163,164]. It is worth noting that often the isotropic chemical shift δ_{iso} shows only a small increase in shielding upon protonation since this information is intrinsically limited by the fact that the changes in δ_{11} and δ_{22} are in opposite directions, while δ_{33} is not particularly influenced.

4.3.4 ^{15}N chemical shift

^{15}N chemical shift probably represents the best parameter for the location of the hydrogen atoms along hydrogen bond contacts involving nitrogen atoms as well as for evaluation of proton transfer occurrence from the acid to the base with formation of charge-assisted contacts. Although its acquisition is hampered by both low gyromagnetic ratio (gamma, γ) value ($-27.126*10^6$ rad s^{-1} T^{-1}) and natural abundance (0.37%) which lead to a dramatic scarce sensitivity ($3.84*10^{-6}$ and $2.25*10^{-2}$ with respect to ^1H and ^{13}C, respectively), the literature is full of ^{15}N SSNMR studies. Of course, as a drawback for natural abundance systems, it requires very long (one or more days or even impractical sometimes) acquisition times to achieve spectra with reasonable S/N ratio. However, ^{15}N chemical shift is more sensitive to the protonation than ^1H due to the wider chemical shift range, and also than ^{13}C since directly involved in the interaction. Indeed, while hydrogen bond formation produces high- or low-frequency shifts from 5 to 50 ppm according to type of nitrogen atom (Scheme 4), the protonation induced shifts that can be as large as 50 ppm or even up to 100 ppm towards lower frequencies for aromatic amines, and up to about 25 ppm towards higher frequencies for aliphatic amines in agreement with the minor contribution of the lone pair to σ^p_{loc} since removed by quaternization [131,165]. A similar effect is observed also upon coordination of the nitrogen atom to metals [166,167].

A general correlation was established between ^{15}N chemical shifts and N···O distances for evaluating proton transfer in crystal acid-base complexes of heterocycles containing nitrogen atoms. This is the case for several acid–base complexes of E-2-Methoxy-N-(3{4-[3-methyl-4-(6-methyl-pyridin-3-yloxyl)-phenylamino]-quinazolin-6-yl}-allyl)-acetamide an ErbB2 inhibitor involving basic aza-heterocycles [168]. The studied crystal structures consisted of the free base, a sesquisuccinic acid cocrystal, a dimalonic acid mixed ionic/zwitterionic complex and a dimaleate salt characterized by N···H···O interactions where the H atoms could be attached to O or N. Small (0.25 Å) changes in the N···O distances caused large low-frequency shift depending on proton transfer: hydrogen bond formation leaded to low-frequency shifts between 20 and 60 ppm, whereas proton transfer shifts greater than 80 ppm.

The ^{15}N solid-state NMR chemical shifts were also instrumental in proving the neutral nature of eight cocrystals between 2-acyl (alkyl in acyl = methyl, ethyl, t-butyl, and 1-adamantyl) amino-6-R-pyridine and 4-R0-benzoic acid (R, R0 = H or Me) [169]. In all structures, the molecules are held together by O-H···N hydrogen bonds between the pyridyl nitrogen atom and carboxylic acid rather than a charge-assisted $^-O···H–N^+$ interactions.

^{15}N spectra were also use to investigate the presence of specific drug − excipient interactions and the occurrence of protonation transfer in amorphous solid dispersions. ^{15}N SSNMR of solid dispersions of Lapatinib, a kinase inhibitors, in HPMCP (hydroxypropylmethylcellulose phthalate) provided direct spectroscopic evidence of the concomitant presence of both ionized and un-ionized Lapatinib [170]. Indeed, the spectra show two signals at -351.7 ppm (typical of the freebase) and at

-335.0 ppm attributed to the Lapatinib phthalate salt. ^{1}H T_1 and ^{1}H $T_{1\rho}$ relaxation studies of the dispersions supported the ionic interaction hypothesis, and confirmed the presence of multiple phases (ionized and neutral) in the cases of excess drug or polymer.

Other interesting cases of drug − excipient interaction have been reported for Vincamine, a poorly soluble natural alkaloid showing several pharmacological properties in relation to neuroprotection, cerebral circulation and on vascular resistance, particularly in the area of blood vessels [171]. Its semi-synthetic derivative, Vinpocetine, was also studied (Scheme 5). The protonation state of Vincamine has been evaluated in the form of "phytocomplex" (as a standardised Vinca minor L leaf dry extract) [172] as well as in different mixtures with both crosslinked polymers such as polyvinylpyrrolidone (PVP-Cl) and croscarmellose sodium (AcDiSol®) [173] and linear polymers such as sodium carboxymethyl cellulose, (NaCMC) and polyvinilpyrrolidone (PVP-K30) [174]. In the case of linear polymers, the mixture consists of a dispersion of drug nanocrystals in the polymer (thus preserving the neutral character), with improved in vitro bioavailability and physical stability.

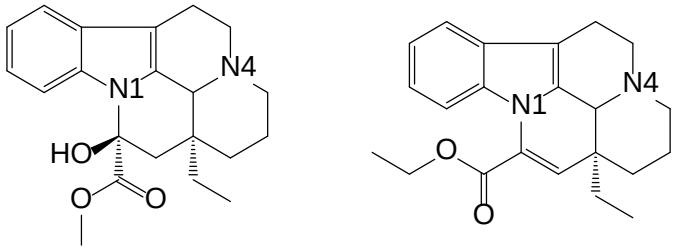

Scheme 5. Chemical structure of Vincamine (left) and Vinpocetine (right) with nitrogen atom label.

In the case of the Vinpocetine, its protonation state has been ascertained by ^{15}N SSNMR in a Vinpocetine-PVP-CL (crospovidone) co-ground mixture in comparison with both pure drug and Vinpocetine citrate salt (Oxopocetine®) (Fig. 7) [175]. The high-frequency shift to 18.8 ppm of the N4 signal in the Vinpocetine-PVP-CL sample with respect to 4.0 ppm of the pure Vinpocetine indicates that the Vinpocetine molecules were protonated as well as in the Oxopocetine® (peak at 19.0 ppm). A similar shift (up to 18.7 ppm) has been observed also when Vinpocetine has been co-crystallized with boric acid providing evidence of salt formation (Fig. 7) [31].

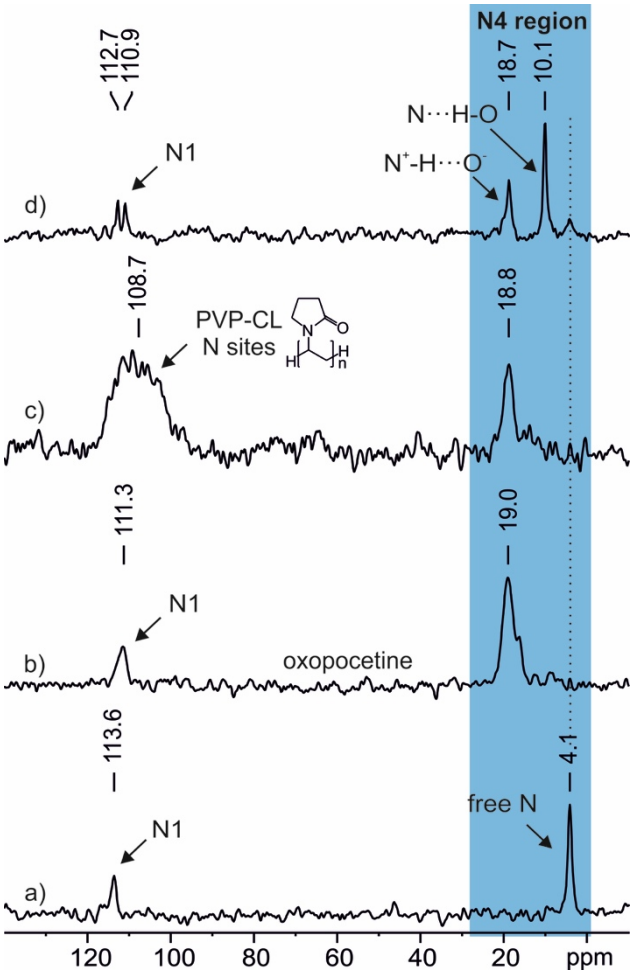

Fig. 7. ^{15}N (40 MHz) CPMAS spectra with relevant assignments of (a) pure Vinpocetine, (b) Oxopocetine ©, (c) 1:1 Vinpocetine-PVP-CL co-ground system and (d) Vinpocetine-boric acid salt. Reprinted in part from ref. [31], Copyright (2016), with permission from Elsevier, and in part from ref. [175], with permission of Springer.

Apart from chemical shift, several advanced techniques have been developed in order to provide insights on proton transfer. Dipolar dephasing experiments (also called non quaternary suppression, NQS, or dipolar interrupted), for instance, provide spectra characterized by non-hydrogenated nitrogen signal only thanks to the presence of a short delay between the cross-polarization and the acquisition period during the pulse sequence. Apperley et al. individuated the site of proton transfer in Sildenafil citrate, the active ingredient of Viagra®, using dipolar dephasing ^{15}N CPMAS NMR spectroscopy [176].

In a similar way the strength of the proton decoupling radio-frequency field during the acquisition can change the intensity of the nitrogen signal according to the presence and number of attached protons. Variankaval and co-workers, for instance, differentiated protonated and non-protonated ^{15}N sites using low power decoupling to eliminate signals effectively from the strongly coupled NH groups [177].

Also the contact time during the CP allows the identification of protonate/non-protonated nitrogen atoms: indeed, short contact times favour ^{15}N atoms directly attached to protons, since characterized by stronger ^{1}H–^{15}N dipolar couplings. This method has been used for the characterization of the acid–base complexes of the ErbB2 inhibitor (see above) [168].

2D SSNMR correlation spectroscopy may also be used to characterize directly molecular association between the ion pair in a salt or the API and coformer in a cocrystal [178]. Proton transfer in acid–base complexes can also be established through dipolar (through space) or scalar (through bond) based 2D experiments. Lesage et al. showed that 2D ^{1}H–^{15}N MAS–J–HMQC NMR spectroscopy can be used to correlate isotropic chemical shifts between pairs of directly bonded ^{1}H and ^{15}N spins, allowing protonated ^{15}N sites to be readily identified [179].

Both direct and indirect acquisition of the ^{14}N isotope rather the ^{15}N one has been proved to be promising in characterized nitrogen environments including its protonation state in both model and real compounds [180–183]. There are inherent difficulties in observing ^{14}N atoms due to limited resolution and sensitivity related to low gamma ($-19.338 \cdot 10^{6}$ rad s^{-1} T^{-1}), large quadrupolar couplings which lead to very broad signals and integer spin quantum number (I = 1) which further complicates the spectra. However ^{14}N nuclei have high isotopic abundance (99.6%) allowing, with MAS rates higher than 60 kHz, acquisitions of solution-like HMQC experiments based on the J-coupling or dipolar interactions which provide further insights on the protonation state of the nitrogen atoms [181,184,185].

^{14}N ultra-wideline (UW), ^{15}N-^{1}H indirect detected HETCOR and ^{15}N dynamic nuclear polarization (DNP) SSNMR experiments, in combination with plane-wave DFT calculations of ^{14}N electric field gradient (EFG) tensors, were used successfully to evaluate the ionic or neutral nature of a series of nitrogen-containing APIs, including HCl salts of Scopolamine (Fig. 8), Alprenolol, Isoprenaline, Acebutolol, Dibucaine, Nicardipine, and Ranitidine [186]. Several types of nitrogen environments, both ionic and neutral pseudotetrahedral sites (i.e., RR'R''NH^{+}, RR'NH_2^{+} and RR'NH) or other sites (i.e., RNH_2 and RNO_2) have been identified and characterized by ^{14}N NMR spectra acquired with special techniques (WURST-CPMG and BRAIN-CP) for overcoming low sensitivity and very large signals. These spectra provided ^{14}N EFG tensor values and orientations that are particularly sensitive to variations in local structure, proton transfer and intermolecular hydrogen bond interactions.

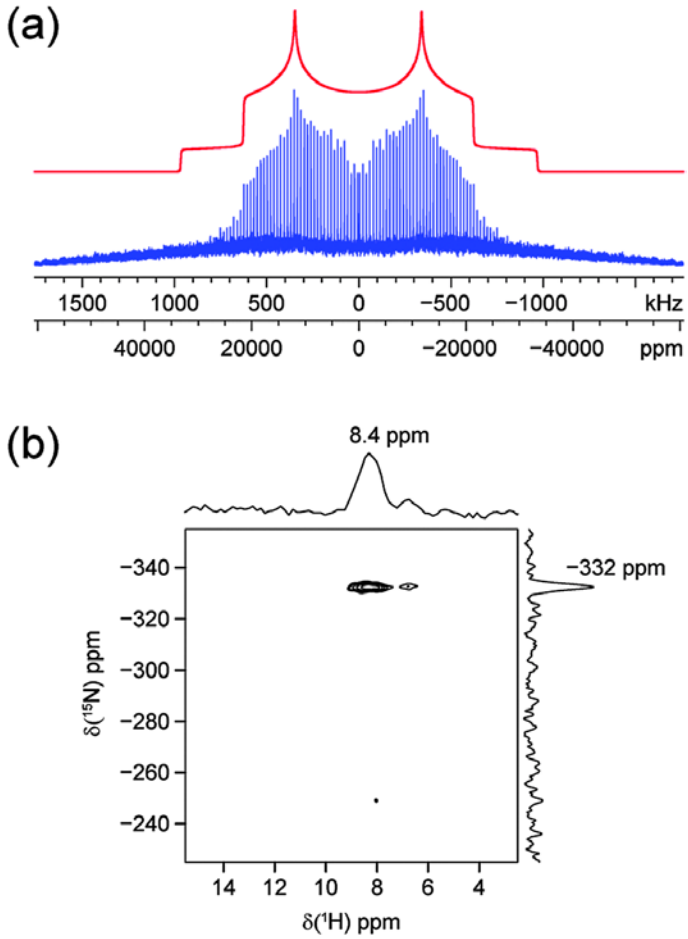

Fig. 8. (a) Static ^{14}N (28 MHz) direct excitation SSNMR spectrum (NH^+ site) and (b) $^{1}H\{^{15}N\}$ (600 and 60 MHz) indirect detection dHETCOR spectrum of Scopolamine hydrochloride salt. The correlation in the indirect detection HETCOR spectrum indicate the salification of the N site. Reproduced from ref. [186] with permission of The Royal Society of Chemistry.

These advanced approaches are promising for elucidating the neutral or ionic nature of multicomponent crystals and in the next future, also thanks to continuous technical and hardware developments and improvements, their systematic application is expected to become routine also for many others pharmaceutical-based crystal forms. ^{15}N solid state NMR has been also proposed as a high sensitive probe for halogen bond detection when a direct nitrogen-halogen interaction is present [187,188].

4.3.5 ^{15}N chemical shift anisotropy

As for ^{13}C, a more accurate approach to establishing the degree of proton transfer in the solid state is to measure chemical shift tensor values. Compared to ^{13}C CSA, dealing with ^{15}N CSA tensors is much more challenging because of the very poor sensitivity of the ^{15}N resonance that makes their measurement highly impractical. Indeed, their achievement usually requires very expensive ^{15}N-enriched samples. The principal values and the orientation of the ^{15}N chemical shift tensors (Scheme 4) could be derived for different classes of nitrogen-containing model compounds such as amine, imine, pyridine-like, pyrazole/imidazole nitrogen atoms. The tensor values were extracted by ^{15}N lineshape simulation of static powder spectra recorded under condition of ^{1}H-^{15}N CP as reported for the acid-base adducts between 2,4,6-trimethylpyridine (collidine) and several benzoic acid derivatives [128].

For heterocyclic nitrogen atoms, the principal CS tensors are labeled also according to the literature as tangential component $\delta_{11} = \delta_t$, radial component $\delta_{22} = \delta_r$ and perpendicular component $\delta_{33} = \delta_\perp$. Solum *et al*. showed that for pyridine and pyridinium the values of δ_t and δ_r are inversed [189–191]. For heterocyclic systems, it has been reported that δ_{22} and δ_{33} are not very sensitive to proton position and hydrogen bond geometry and move towards one another whereas δ_{11} is strongly shifted to lower frequencies when the proton atom approaches nitrogen site [192]. Concerning amide groups in crystalline histidine and histidine-containing peptides, systematic trends in values of imidazole CSA with changes in hydrogen bonds has been documented. A correlation was found between the ^{15}N δ_{11} tensor value and the hydrogen bond length for cationic species. As the hydrogen bond distance decreases, the δ_{22} tensor value shifts toward higher frequencies.

4.4 Computational Density Functional Theory Studies

The increasing ability to relate chemical shifts as well as the tensor components to the crystallographic location of relevant atoms in the unit cell via computational methods has added significantly to the practice of NMR crystallography. In this sense, computational methods are becoming increasingly fundamental in supporting and assisting the interpretation of experimental SSNMR data. Such computations are commonly carried out within the well-established DFT calculation, using the plane waves approach as implemented in the gauge-including projected augmented wave (GIPAW) method [193,194]. Although the earlier developed gauge-including atomic orbitals (GIAO) method is still popular among SSNMR users [29,195,196], the GIPAW approach makes it possible to include the whole crystalline unit cell into calculation, thus accounting for the periodicity of a crystal which provides accurate results when strong intermolecular interactions are present [197,198]. DFT-D approaches were also implemented which correct the DFT energy for dispersion effects providing a better description of the non-covalent interactions with a reasonable compromise between precision, simplicity, and computational cost [199]. The synergy between experimental data and quantum chemical computations enables excellent structure prediction: for instance, NMR crystallography allows for an accurate localization of hydrogen atoms in hydrogen bond networks [200]. For this reason, the proton CSA has been successfully used as a sensitive probe to determine the packing interactions present in the supramolecular arrangements of both organic and inorganic solids [201–203]. Likewise, chemical shift parameters of other nuclei such as ^{13}C and ^{15}N are also important to gain structural information [93,204,205].

The Furosemide-Isonicotinamide cocrystal represents an interesting example were DFT calculations using the GIPAW method implemented in CASTEP v6.0 [193,194,206] helped in determining the neutral nature of the multicomponent crystal form. Indeed, while the proton transfer from Furosemide to Isonicotinamide would result in a ^{15}N signal around -152.3 ppm, the observed chemical shift at -116.0 ppm accounts for a neutral O-H···N interaction supporting the XRD data [207].

DFT calculations were carried out also to check the ionic or neutral nature of 8-Chlorotheophylline inside Dimenhydrinate [140], a multicomponent drug for the prevention of motion sickness, including nausea and vomiting. The DFT calculations were carried out to obtain an optimized structure of both species, salt and cocrystal. A close inspection of several atom distances in the neutral and in the ionic computed structures strongly supported the experimental SCXRD structure that the 8-Chlorotheophylline is protonated and Dimenhydrinate drug exists as salted form.

4.5 X-ray photoelectron spectroscopy (XPS)

XPS, like SSNMR, probes the chemical environment of individual atoms. It is a surface-sensitive technique (e.g., the N 1s photoemission results from an approximate signal probing depth of 5–9 nm) [208,209] that can provide molecular information on trace quantities of material localized at a surface. The chemical shifts in XPS depend on the chemical environment, as differing amounts of energy (binding energy, E_B) are required to emit an electron from an atomic core level [210–212]. In this sense, XPS is sensitive to the protonation state of N atoms as well as to their environments (e.g. hydrogen bonding). For example, the nitrogen salification will cause a shift of the N 1s peak in the emission spectrum. The ability of XPS to determine the presence of protonated versus unprotonated nitrogen in pharmaceutical salts and cocrystals has been demonstrated with N 1s chemical shifts [209,211].

For instance, combined ^{15}N SSNMR and XPS investigations for Theophylline, an oxalic acid·Theophylline cocrystal, and a 3-sulfosalicylic acid·theophyllinium salt demonstrated that XPS allows direct observation of the degree of proton transfer, and thus identification of whether a salt or a cocrystal has been formed [209]. Indeed, in the case of the salt, a strong chemical shift of +2.3 eV towards higher binding energy has been observed indicating the acquisition of a strong positive charge localised at the purinic nitrogen atom (N9) (Fig. 9). This unambiguously confirms formation of a salt with a $C=NH^+$ moiety, in agreement with the distances observed in the crystal structure. On the other hand, the N 1s emission spectrum of the cocrystal between Theophylline and oxalic acid was identical to that of pure Theophylline in agreement with the presence of a neutral C=N moiety.

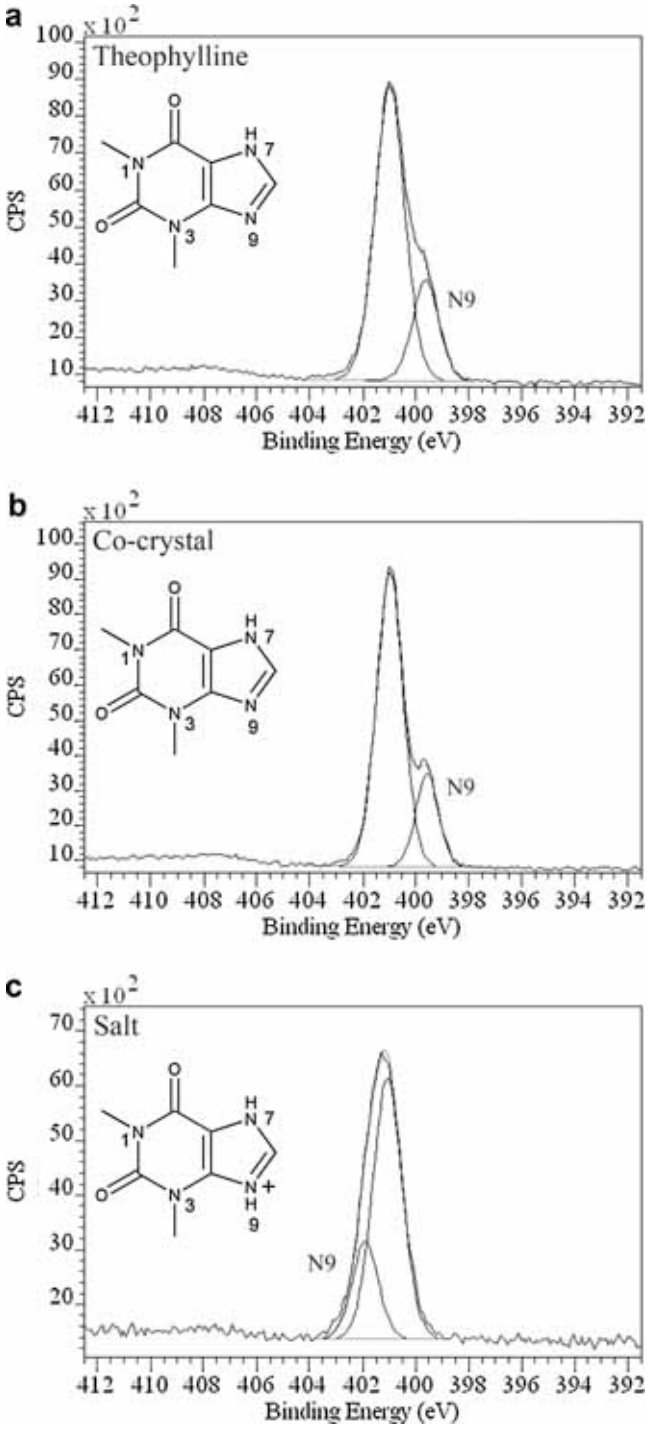

Fig. 9. XPS N 1s spectra of (a) Theophylline, (b) 2:1 Theophylline–oxalic acid co-crystal, and (c) theophyllinium salicylic-5-sulfonate monohydrate salt. Reprinted from ref. [208], Copyright (2016), with permission from Elsevier.

Again, XPS was used combined with ^{15}N SSNMR to investigate the drug-excipient interactions in amorphous solid dispersions of polystyrene sulfonic acid (PSSA) and two weakly basic anticancer drugs, Lapatinib and Gefitinib [213]. The binding energy increases detected by XPS in the basic nitrogen atoms in both Lapatinib and Gefitinib, strongly indicated protonation of these nitrogen atoms. On the other hand, ^{15}N SSNMR provided direct evidence for protonation of the quinazoline nitrogen atoms in both APIs, as well as the secondary amine nitrogen atom in Lapatinib and the tertiary amine nitrogen atom in Gefitinib.

In a similar way, XPS was recently instrumental for discovering the source of discoloration in a pharmaceutical fumarate salt with compromised mechanical properties [214]. Adhesion of the N free base to the surface of the fumarate salt was ascertained through analysis of NH^+/N peak ratios in the N 1s XPS emission spectra.

5. Selected examples

The great interest of researchers for new salts and cocrystal of APIs is witnessed by the large number of publications that appeared in the scientific literature in recent years. We would like to present here a few selected examples published in the last five years with a particular attention on topical contributions devoted to tackling the characterization challenges.

5.1. Salts

Agomelatine (AG) is an API used as an antidepressant drug with moderate agonistic action at the melatonine receptor MT1 and weak effect at MT2, discovered and developed by Servier Laboratories with first marketing approval in 2009 [215]. AG has several different polymorphs with the crystal form I and II mainly used in pharmaceutical industry [216]. Moreover, many other solvate and cocrystal stuctures are reported in the literature [217]. AG represents an interesting case-study to understand if the reported forms are salts or rather cocrystals. The molecule of AG does not contain any traditionally accepted ionizable functional groups. Recently E. Skořepová and coworkers were able to synthesize three novel solid forms in the presence of partially oxidized hydriodic acid leading to three salts with different iodine ratio (AGI, AG_2I_3 and AGI_2) with the molecules of AG protonated on the amidic oxygen [218]. The protonation states of AG iodides were obtained by SCXRD (Scheme 6) and ^{13}C (Fig. 10) and ^{15}N (Fig. 11) solid state NMR data.

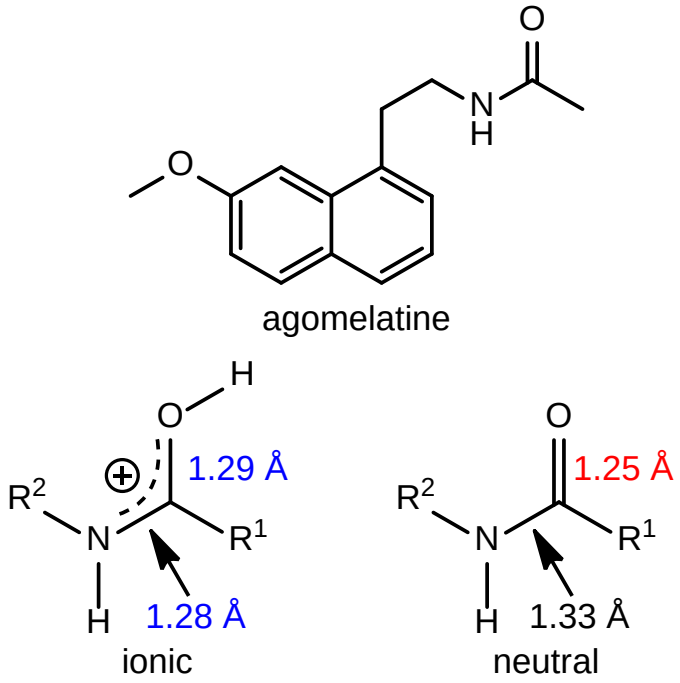

Scheme 6. Chemical structure of AG (top) with relevant C-O and C-N bond lengths in a neutral molecule (bottom right, values for AG polymorph II) and a salt (bottom left, values for AGI) as observed by XRD.

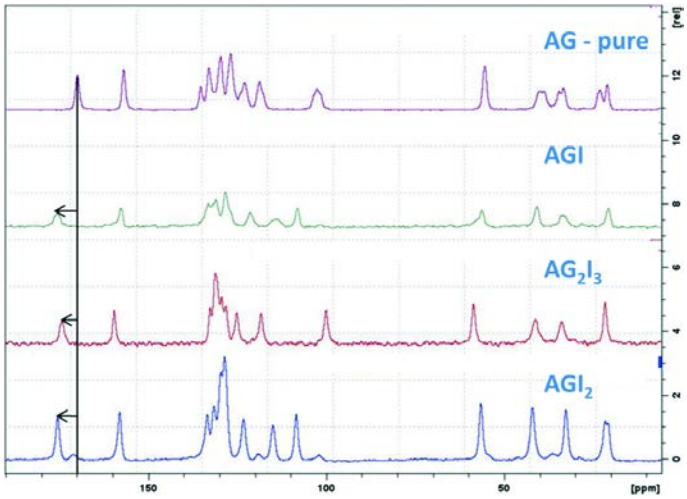

Fig. 10. ^{13}C (100 MHz) CPMAS SSNMR of AG solid forms, top to bottom: AG polymorph I, AGI, AG_2I_3 and AGI_2. The change in the chemical shift of the carbonyl signal is highlighted. Reproduced from ref. [218] with permission of The Royal Society of Chemistry.

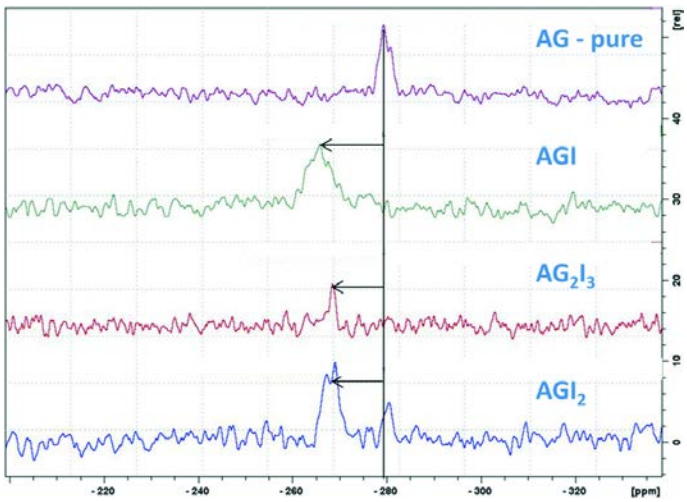

Fig. 11. ^{15}N (40 MHz) CPMAS SSNMR of AG solid forms, top to bottom: AG polymorph I, AGI, AG_2I_3 and AGI_2; the change in the chemical shift of the amidic nitrogen atom is highlighted. Reproduced from ref. [218] with permission of The Royal Society of Chemistry.

The change in the chemical shifts of amidic carbon and nitrogen observed on the ^{13}C and ^{15}N spectra for the iodide derivatives compared to the pure AG (polymorph I) is a clear indication of the protonation of the amidic oxygen. Therefore, all three AG iodides have a salt character. The change in the chemical shift is distinctly larger for AGI than AG_2I_3 and AGI_2, in agreement with a formal charge of +1 for AGI, and +1/2 for AG_2I_3 and AGI_2, as the last two show symmetric hydrogen bond and $[AG_2H]^{+1}$ complexes in their structures.

5.2 Salt cocrystals (SCCs)

Cocrystals of Erlotinib (a drug used for the treatment of non-small cell lung cancer) with urea, succinic acid, and glutaric acid and salts with maleic acid, adipic acid, and saccharin were prepared via wet granulation and solution crystallizations [219]. The new solid forms characterized by PXRD show that self-recognition via the (amine) N-H···N (pyridine) hydrogen bond between the API

molecules is replaced by several heterosynthons such as acid-pyridine, amide-pyridine and carboxylate-pyridinium in the new binary systems. The authors highlight that auxiliary interactions play an important role in determining the conformation of the API in the crystal.
Cocrystal derivatives of Tenoxicam (Scheme 7), a member of the oxicam class non-steroidal anti-inflammatory drugs (NSAID), have been reported in order to enhance the poor solubility of the API. The weak acidity of Tenoxicam (pK_a = 5.1), represents an intrinsic limitation of the number of counter-ions able to form stable, pharmaceutically-acceptable salts [220].

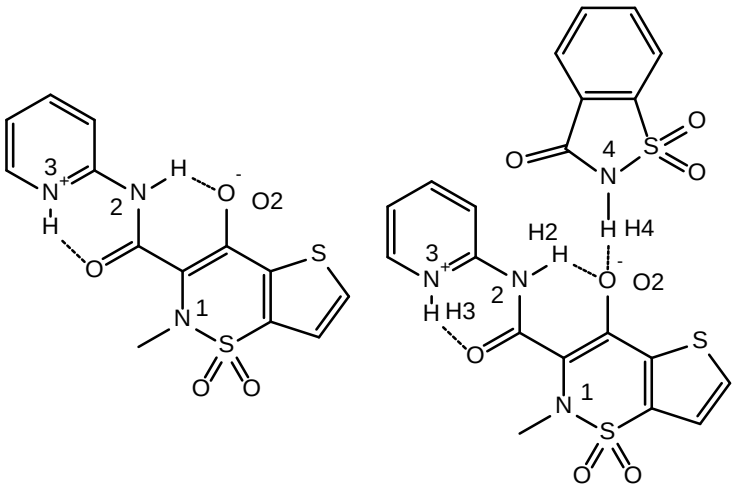

Scheme 7. Chemical structure of Tenoxicam (left) and Tenoxicam-saccarine cocrystal (right) with relevant atom labels and hydrogen bonds.

By combining information from DSC, SSNMR spectroscopy and PXRD, Vogt and coworkers [221] were able to fully characterize nine different Tenoxicam cocrystals together with the presence of solvates and phase mixtures. 2D SSNMR methods have been employed to confirm cocrystal formation and determine structural aspects for cocrystals with saccharin, Salicylic acid, succinic acid, and glycolic acid in comparison to Forms I and III of the API. Weak interactions have been detected by ^{1}H–^{13}C HETCOR and ^{1}H double-quantum (DQ) MAS experiments, whereas ^{15}N SSNMR measurements were useful to assess the ionization state in cocrystals (Fig. 12).

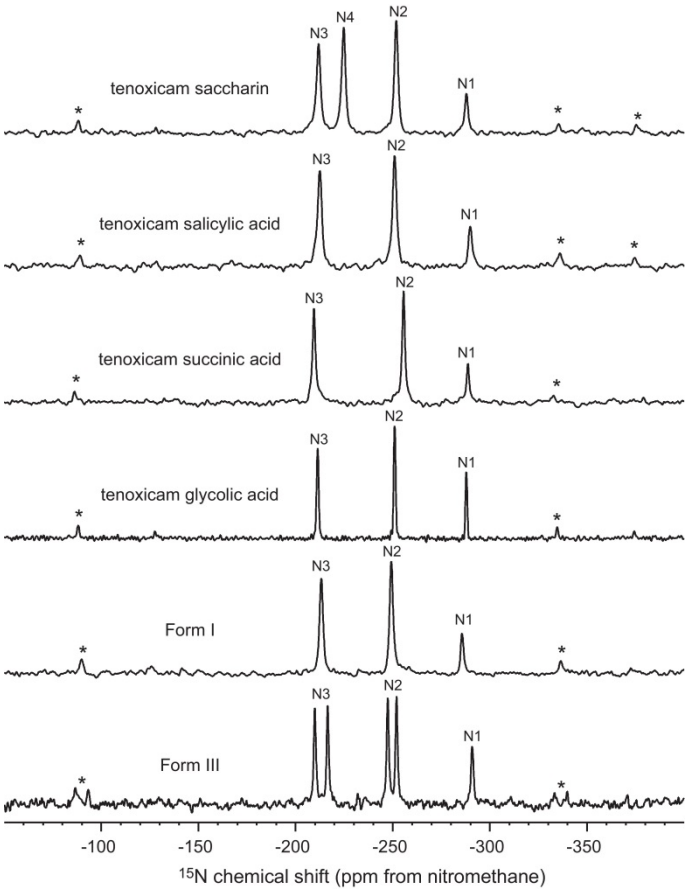

Fig. 12. ^{15}N (40 MHz) CPMAS spectra (spinning speed = 5 kHz, 273 K) of cocrystals of Tenoxicam with saccharin, Salicylic acid, succinic acid, and glycolic acid. The ^{15}N CPMAS spectra of the polymorphs of Tenoxicam (Forms I and III) are shown for comparison. Asterisks denote spinning sidebands. Reprinted from ref. [221], Copyright (2012), with permission from Elsevier.

Form III of pure Tenoxicam is known from SCXRD to be zwitterionic, with protonation at N3 and deprotonation at O2 and the presence of two independent molecules in the crystallographic cell [222,223]. Accordingly, ^{15}N NMR spectrum of form III shows a peak splitting for the N2 and N3 resonances. Based on ^{15}N SSNMR data, all other forms, form I and the other cocrystals, display the same zwitterionic character as that in Form III. The ^{1}H DQ-BABA spectrum of the Tenoxicam saccharin cocrystal (Fig. 13) shows a strong interaction with a DQ frequency of 27 ppm between the most deshielded peak, assigned to N3H, and N4H, providing direct evidence of association between Tenoxicam and saccharin also in this case in which no SCXRD data are available.

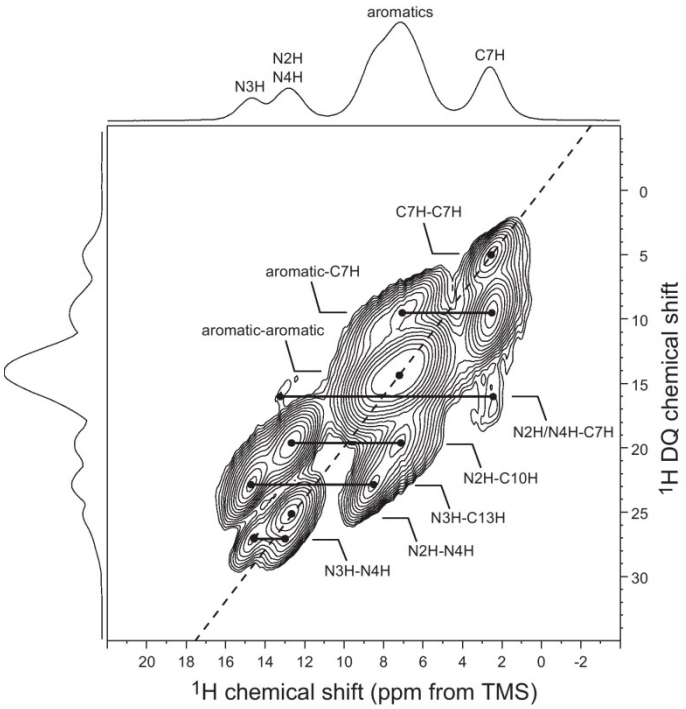

Fig. 13. ^{1}H (500 MHz) DQ-BABA spectrum (spinning speed = 35 kHz, 273 K) of Tenoxicam·saccharin. The ^{1}H MAS spectrum is plotted along the F2 (horizontal) axis and a double quantum skyline projection is shown along the F1 (vertical) axis. Several key correlations are noted on the spectrum. Reprinted from ref. [221], Copyright (2012), with permission from Elsevier.

Nangia and coworkers [224] reported the synthesis and characterization of cocrystals of Tenoxicam with coformers of the FDA GRAS list of pharmaceutically acceptable compounds such as benzoic acid, Salicylic acid, catechol, resorcinol, and pyrogallol and salts with Piperazine, hydrochloride, and methanesulfonic acid. Two coformers of the zwitterionic form of Tenoxicam are present in the crystal structures (Fig. 14), both showing intramolecular proton transfer from the enolic OH to the pyridine nitrogen.

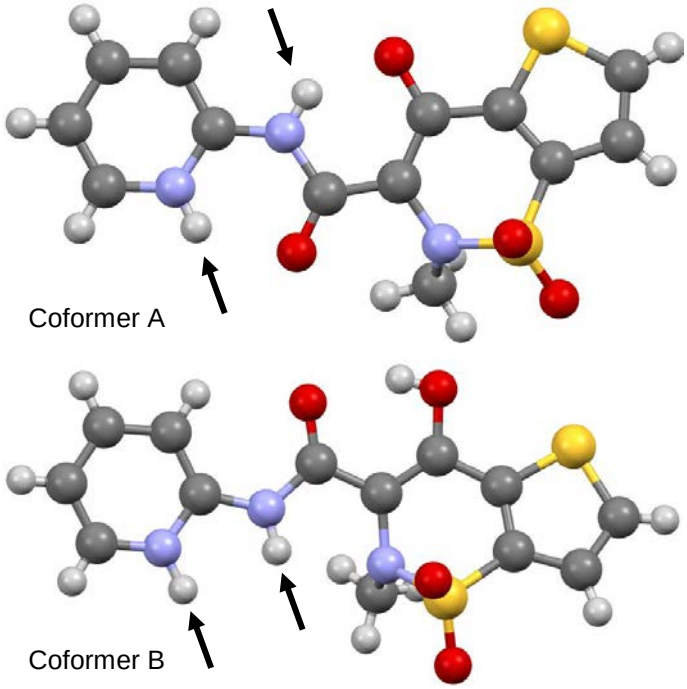

Fig. 14. The two possible coformers observed for Tenoxicam. Coformer A is present in Tenoxicam, all solvates, and cocrystals with moderate acids. Coformer B exists in Tenoxicam·HCl and Tenoxicam·methanesulfonic acid salts. Adapted with permission from ref. [224]. Copyright (2013) American Chemical Society.

Coformer A is formed when the pyridinium N^+-H and amide N^--H are in *anti* position, whereas in coformer B they are *syn* oriented. By X-ray crystal structure determination the coformer A is found on cocrystals of Tenoxicam with benzoic acid, Salicylic acid, catechol, resorcinol, and pyrogallol and salts with Piperazine, whereas coformer B is present in the salts with HCl and methanesulfonic acid.

The resorcinol and the pyrogallol cocrystals showed 10.1 and 7.5 times higher solubility than pure teboxicam in a pH 7 buffer medium, with a good correlation between the solubility of Tenoxicam cocrystals with the solubility of the coformer. Slurry experiments in the acidic medium suggest that the carboxylic acid cocrystals are stable, whereas the salts are unstable with the counterions that are protonated in the acidic medium to release the API, which then decomposes in its native state.

A paradigmatic case of how the formation of an API cocrystals is able to modify physicochemical properties of the API has been reported by Ramanan and coworkers in 2013 [225]. The authors were able to crystallize p-Aminosalicylic acid (PAS), a well-known antibiotic in tuberculosis treatment and also a promising anticancer drug [27,226–230] in the presence of pyridine derivatives as coformers, thus obtaining nine multicomponent solids that include salts, cocrystals, SCCs/SCCs hydrates and cocrystal polymorphs. Salt-cocrystal continuum cannot be ruled out in some of the presented cases. $COOH\cdots N_{heterocycle}$ synthon is responsible for the multiple forms of the drug molecule with pyridine and bpy based coformers. Interestingly, the same $COOH\cdots N_{heterocycle}$ synthon was found to be the driving force also for the formation of PAS-Isoniazid and PAS-Pyrazinamide drug-drug cocrystals used in first-line treatment to prevent multiple drug-resistant tuberculosis [231].

Depending on the solvent of crystallization and the API-coformer composition in solution, several crystal forms were synthesized (Scheme 8): cocrystals of PAS with bipyridine (2:1 and 2:3), 1:2

SCC monohydrate of PAS and bypiridine, 1:1 salt of PAS and 4-aminopyridine, salt of PAS and 3-hydroxypyridine, 2:1 salt of PAS and 1,2-bis(4-pyridyl)ethane, two polymorphs of 1:1 cocrystal of PAS and 1,2-bis(4-pyridyl)ethane, and 1:1 cocrystal of PAS and 1,2-bis(4-pyridyl)- ethylene. The stretching mode of carbonyl groups has been used to confirm the formation of cocrystals or salts: an intense band related to free carboxylic acid is found for cocrystals, confirming the presence of neutral species in these solid forms, whereas the same band is weak in salts.

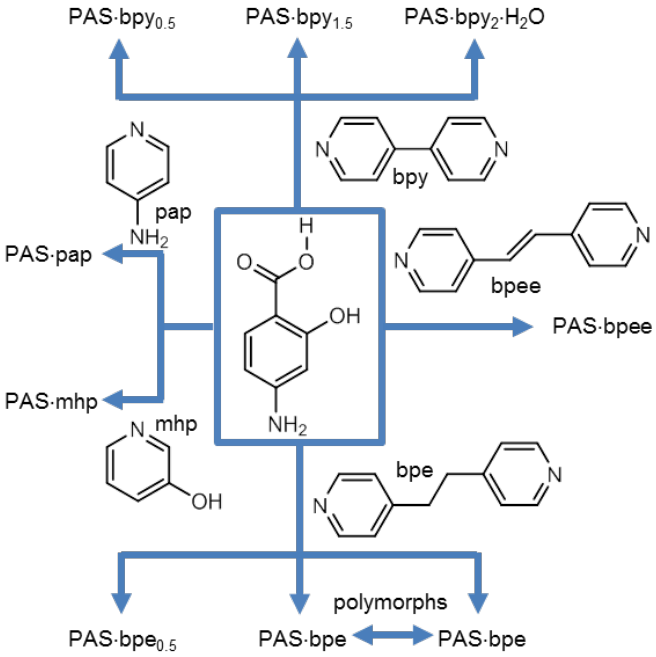

Scheme 8. Co-crystallization of p-Aminosalicylic Acid (PAS) with different coformers under varying composition and solvent; bipyridine (bpy), 4-aminopyridine (pap), 3-hydroxypyridine (mhp), 1,2-bis(4-pyridyl)ethane (bpe), 1,2-bis(4-pyridyl)- ethylene (bpee).

Niclosamide (2,5-dichloro-4-nitrosalicylanilide), (HNic), is an API which belongs to the Salicilamide class and is the only commercially available antihelmintic for humans and animals to be recommended by the WHO (World Health Organization) for large scale use in schistosomiasis control programs [232]. One anhydrous and two different hydrate HNic forms have been reported in the literature [233]. Several cocrystals with Caffeine, urea, and Theophylline, have also been reported [234]. Recently, four new SCCs (KNic·HNic·H_2O, KNic·HNic·$3H_2O$, NaNic·HNic·$3H_2O$, NaNic·HNic·$2H_2O$), a classic cocrystal with imidazole (IM) (HNic·IM), and two sodium salts, (NaNic·DMSO·H_2O and NaNic·DMSO·$2H_2O$) have been reported by some of us [11]. All samples have been investigated using a combination of solid-state experimental techniques such PXRD, SSNMR, IR, and Raman which provide complementary information on powdered samples. The peculiarity of these SCCs is the API's concomitant presence as both a neutral component and as a salt coformer, and the fact that they interact via hydrogen bonding. Single crystals were only obtained for KNic·HNic·H_2O (Fig. 15) and NaNic·DMSO·$2H_2O$ (Fig. 16). The nature of the adducts (whether salt or cocrystal), their stoichiometry and the presence of independent molecules in the unit cell of the other samples were thus all determined by means of SSNMR and the comparative analysis of ^{13}C, ^{15}N CPMAS, and ^{1}H MAS spectra. Furthermore, DSC, TGA and intrinsic dissolution rate measurements completed the characterization and enabled to evaluate the effects of microscopic changes (molecular packing, weak interactions, conformations, etc.) on the

macroscopic properties (thermal stability and bioavailability) of the multicomponent forms. The results obtained indicate that the formation of SCCs provides a reliable method whereby the HNic intrinsic dissolution rate improves.

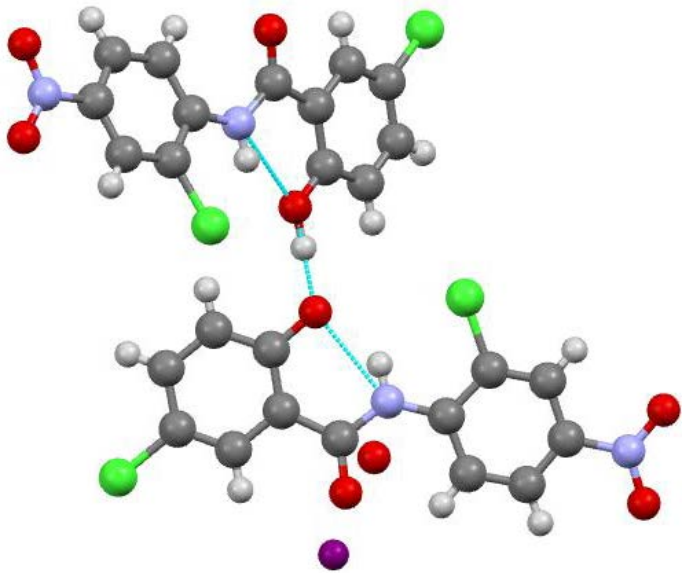

Fig. 15. Crystal structure of KNic·HNic·H_2O: highlighting the short hydrogen bond between the HNic and Nic^- forming a dimer. The hydrogen atoms of the water molecules are omitted. (K^+ ion in violet). Adapted with permission from ref. [11]. Copyright (2015) American Chemical Society.

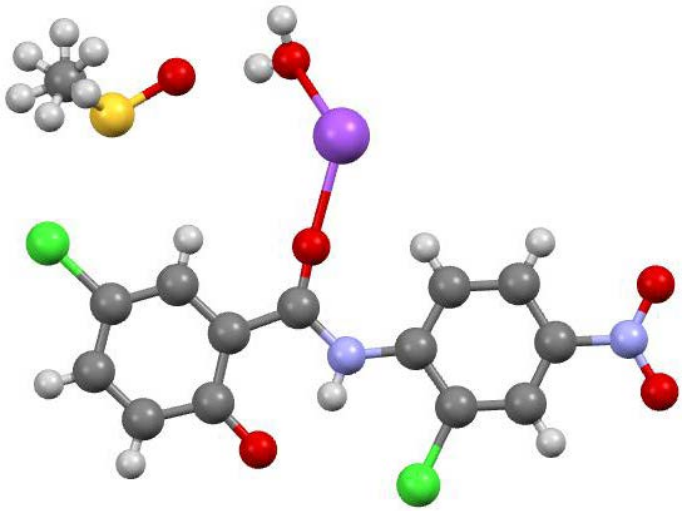

Fig. 16. Asymmetric unit of NaNic·DMSO·$2H_2O$ with the molecule of Nic^- and the Na^+ lying on a mirror plane, as well as the sulfur and the oxygen of the DMSO molecule. (K^+ ion in violet). Adapted with permission from ref. [11]. Copyright (2015) American Chemical Society

The crystal structure of the 1:1 benzamide cocrystal of Theophylline, was determined from a combination of SSNMR and synchrotron PXRD data [235]. Based on the comparison of ^1H chemical shift of the 1:1 benzamide cocrystal of Theophylline (13.4 ppm) with respect to the pure coformers (Fig. 17) it is evident that the proton is bridged weaker to benzamide in the cocrystal as in pure Theophylline, in agreement with the presence of neutral molecules without proton transfer. The possibility of salt formation was ruled out also by Raman spectroscopic analysis that shows

stretching band shifts of only 5 cm^{-1} in the cocrystal. Peak splitting in the ^{13}C CPMAS NMR spectrum confirms the presence of more than one independent molecule in the cocrystal lattice. Structure determination by synchrotron PXRD data was not an easy task, though the authors were eventually able to determine that the cocrystal crystallizes in the tetragonal space group $P4_1$ with four independent molecules in the asymmetric unit. The crystal structure was confirmed by dispersion-corrected DFT calculations including an optimization of the lattice parameters.

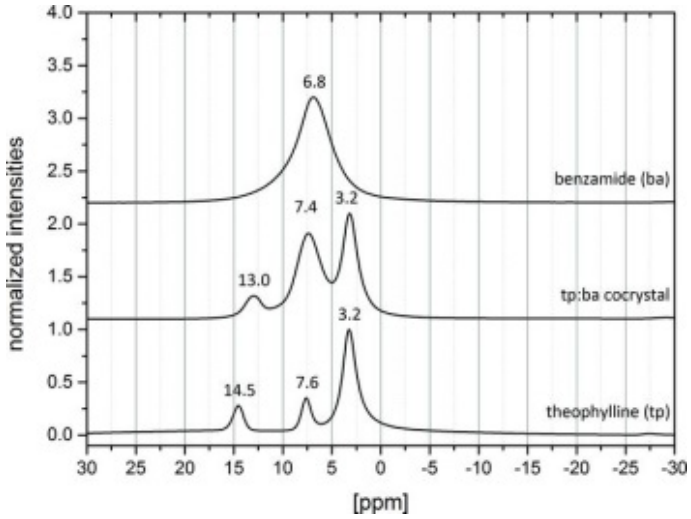

Fig. 17. ^{1}H (600 MHz) MAS NMR spectra of Theophylline (tp),·benzamide (ba) and Theophylline·benzamide (tp:ba) cocrystal acquired with a spinning speed of 25 kHz. Reproduced from ref. [235], Copyright (2016), with permission of the International Union of Crystallography. http://journals.iucr.org/

5.3. Ionic cocrystals (ICCs)

ICCs involving organic molecules and metal halides has been successfully employed for solid formulation of API's [12–14,16,236–239]. In these compounds the organic molecule acts as a sort of special solvent towards the metal cation. Interestingly, it was generally found that ICCs have higher solubility than neutral cocrystals, and extremely variable coordination numbers and geometries are observed for alkaline and alkaline earth metal coordination. Often single crystals are difficult to grow, or the products are obtained by mechanical mixing of the reactants, thus structure solution from powders becomes necessary.

Halogen atoms are frequently present in drug molecules and can be used to drive the formation of pharmaceutical cocrystals if halogen bonding is used [240,241]

The first example of the use of halogen bond for obtaining pharmaceutical cocrystals of a halogenated API has been recently reported by some of us [242]. Four pharmaceutical cocrystals of 3-Iodo-2-propynyl-n-butylcarbamate (IPBC) (Scheme 9), an iodinated antimicrobial product used globally as a preservative, fungicide, and algaecide, have been synthesized and fully characterized with various techniques demonstrating that halogen bond is the key interaction responsible for the self-assembly of the reported pharmaceutical cocrystals. Two bipyridine derivatives as neutral acceptors of halogen bond (1,2-Bis(4-pyridyl)ethane and 4,4′-Bipyridine), and two halide ions, as anionic acceptors of halogen bond (tetra-n-butylammonium iodide and $CaCl_2$) have been selected.

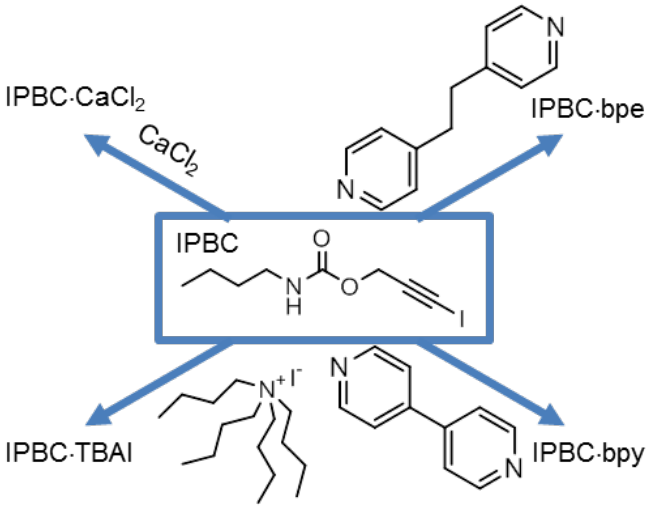

Scheme 9. Molecular structures of IPBC (3-Iodo-2-propynyl-n-butylcarbamate) with 4,4′-Bipyridine (bpy), 1,2-Bis(4-pyridyl)ethane (bpe), tetra-n-butylammonium iodide (TBAI) and calcium chloride ($CaCl_2$).

The 1-iodoalkyne moiety forms very stable cocrystals with both neutral and anionic halogen bond -acceptors. It is worth noting that, in the reported cocrystals, halogen bond does not interfere with the hydrogen bond pattern of the carbamate moiety of IPBC, which remains very much intact. This is important because of the complexity of chemical structures of APIs, which embody a particularly great challenge when design and preparation of specific multicomponent crystals are pursued. Most of the cocrystals described showed improved properties with respect to the source API, in terms, e.g., of powder flow properties and thermal stability. The cocrystal of IPBC with $CaCl_2$, in particular, involving a GRAS cocrystal widely used as dehydrating excipient, has serious possibilities of technological exploitation [243]. The measurement of the angle of repose of its powders has confirmed that cocrystal IPBC·$CaCl_2$ has superior free-flow characteristics compared to the pure IPBC. This strategy is, in principle, applicable to any APIs featuring the iodoalkyne moiety. The results may pave the way toward the extensive use of halogen bond to contribute to improved drug product performance (e.g., solubility, dissolution).

1:1 monohydrate SCC of Gefitinib (Fig. 18) [244], an anticancer drug, and Furosemide [245], a loop diuretic drug, has been prepared and fully investigated by solid-state characterization methods [246]. The Gefitinib–Furosemide molecular salt has some interest due to its potential application in a combination drug therapy. XRD structure shows that proton transfer has occurred from the COOH group of Furosemide to the morpholine moiety of Gefitinib suggesting the formation of a salt cocrystal. Crystal structure analysis revealed that also N–H···O, C–H···O, O–H···N, and O–H···O interactions with a water molecule and π-stacking interaction of the benzene rings are playing a role in the crystal lattice that led to the compact crystal packing, better density, and high thermal stability.

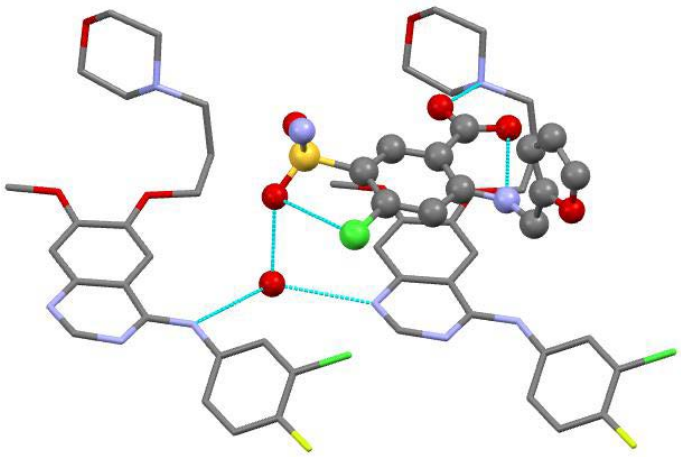

Fig. 18. Crystal structure of the 1:1 monohydrate SCC of Gefitinib (capped stick) and Furosemide (ball and stick). Hydrogen atoms are omitted for clarity. Reprinted from ref. [246], Copyright (2015), with permission from Elsevier.

Solubility and dissolution rate of Gefitinib in the molecular salt hydrate are lower as compared with its stable polymorph which shows a high residence time of the drug at the site of the action. In contrast, substantial increase in the solubility and dissolution rate in the molecular salt are found for the Furosemide with respect to its stable polymorph.

CONCLUSIONS

The efficiency of the orally administered drug products delivered as solid dosage forms are strictly dependent on their solubility into the biological fluids secreted in the gastrointestinal tract and permeation across the gastrointestinal membrane. In order to improve the efficiency a large array of new salt and cocrystal forms of APIs have been developed by enhancing key physicochemical properties such stability, solubility, dissolution rate, bioavailability and pharmacokinetics as well as thermal stability and compressibility without changing the pharmacological nature of the drug.
The scientific literature has witnessed an increasing number of contributions of new researchers in this field coupled with systematic commercialization of salts and cocrystals of APIs with advantageous clinical safety and performance. New synthetic strategies and the full exploitation of the new knowledge on crystal engineering contributed to such growth. Nevertheless there is still a need for a deeper knowledge of the nature of the solid-state forms since an XRD approach is not always able to fully solve the solid structure and must be often coupled with complementary characterization techniques. We presented here the state-of-the-art of the field particularly focusing on the characterization challenges encountered when crystal structure determination often does not afford accurate proton positions. Several paradigmatic examples of the salts and cocrystals of important API that appeared in the literature in the last five years have been presented. We can be confident to predict that in the coming years, such field will continue to grow rapidly and more pharmaceutical salt and cocrystal drug substances will become candidates for a broader commercialization.

ACKNOWLEDGEMENTS

P. C. V. thanks the Istituto Nazionale della Previdenza Sociale (INPS) for a scholarship. We thank each and every student that was involved in the research and development of the projects described above over the past several years. The authors are indebted with Jeol Company for helpful technical assistance and cooperation. The authors would like to thank Simone Bordignon for helpful discussions.

References

[1] D. Taylor, The Pharmaceutical Industry and the Future of Drug Development, in: R.E. Hester, R.M. Harrison (Eds.), Pharmaceuticals in the Environment, The Royal Society of Chemistry, Cambridge, 2015: pp. 1–33.

[2] L. Almeida e Sousa, S.M. Reutzel-Edens, G.A. Stephenson, L.S. Taylor, Supersaturation Potential of Salt, Co-Crystal, and Amorphous Forms of a Model Weak Base, Cryst. Growth Des. 16 (2016) 737–748. doi:10.1021/acs.cgd.5b01341.

[3] S. Domingos, V. Andre, S. Quaresma, I.C.B. Martins, M. Fatima Minas da Piedade, M.T. Duarte, New forms of old drugs: improving without changing, J. Pharm. Pharmacol. 67 (2015) 830–846. doi:10.1111/jphp.12384.

[4] J.M. Miller, B.M. Collman, L.R. Greene, D.J.W. Grant, A.C. Blackburn, Identifying the stable polymorph early in the drug discovery-development process, Pharm. Dev. Technol. 10 (2005) 291–297. doi:10.1081/PDT-200054467.

[5] D.P. Elder, R. Holm, H.L. de Diego, Use of pharmaceutical salts and cocrystals to address the issue of poor solubility, Int. J. Pharm. 453 (2013) 88–100. doi:10.1016/j.ijpharm.2012.11.028.

[6] N. Schultheiss, J.-O. Henck, Role of Co-crystals in the Pharmaceutical Development Continuum, in: J. Wouters, L. Quéré (Eds.), Pharmaceutical Salts and Co-Crystals, Royal Society of Chemistry, Cambridge, 2011: pp. 110–127.

[7] N. Blagden, S.J. Colesb, D.J. Berry, Pharmaceutical co-crystals - are we there yet?, CrystEngComm. 16 (2014) 5753–5761. doi:10.1039/c4ce00127c.

[8] R. Thakuria, A. Delori, W. Jones, M.P. Lipert, L. Roy, N. Rodriguez-Hornedo, Pharmaceutical cocrystals and poorly soluble drugs, Int. J. Pharm. 453 (2013) 101–125. doi:10.1016/j.ijpharm.2012.10.043.

[9] V.K. Parmar, S.A. Shah, Hydrochloride salt co-crystals: preparation, characterization and physicochemical studies, Pharm. Dev. Technol. 18 (2013) 443–453. doi:10.3109/10837450.2012.696270.

[10] K. Gaglioti, M.R. Chierotti, F. Grifasi, R. Gobetto, U.J. Griesser, D. Hasa, D. Voinovich, Improvement of the water solubility of tolfenamic acid by new multiple-component crystals produced by mechanochemical methods, CrystEngComm. 16 (2014) 8252–8262. doi:10.1039/c4ce00549j.

[11] F. Grifasi, M.R. Chierotti, K. Gaglioti, R. Gobetto, L. Maini, D. Braga, E. Dichiarante, M. Curzi, Using Salt Cocrystals to Improve the Solubility of Niclosamide, Cryst. Growth Des. 15 (2015) 1939–1948. doi:10.1021/acs.cgd.5b00106.

[12] D. Braga, F. Grepioni, L. Maini, S. Prosperi, R. Gobetto, M.R. Chierotti, From unexpected reactions to a new family of ionic co-crystals: the case of barbituric acid with alkali bromides and caesium iodide, Chem. Commun. 46 (2010) 7715–7717. doi:10.1039/c0cc02701d.

[13] D. Braga, F. Grepioni, G.I. Lampronti, L. Maini, A. Turrina, Ionic Co-crystals of Organic Molecules with Metal Halides: A New Prospect in the Solid Formulation of Active Pharmaceutical Ingredients, Cryst. Growth Des. 11 (2011) 5621–5627. doi:10.1021/cg201177p.

[14] D. Braga, F. Grepioni, L. Maini, D. Capucci, S. Nanna, J. Wouters, L. Aerts, L. Quere, Combining piracetam and lithium salts: ionic co-crystals and co-drugs?, Chem. Commun. 48 (2012) 8219–8221. doi:10.1039/c2cc33855f.

[15] F. Grepioni, J. Wouters, D. Braga, S. Nanna, B. Fours, G. Coquerel, G. Longfils, S. Rome, L. Aerts, L. Quere, Ionic co-crystals of racetams: solid-state properties enhancement of neutral active pharmaceutical ingredients via addition of Mg2+ and Ca2+ chlorides, CrystEngComm. 16 (2014) 5887–5896. doi:10.1039/c4ce00409d.
[16] A.J. Smith, S.-H. Kim, N.K. Duggirala, J. Jin, L. Wojtas, J. Ehrhart, B. Giunta, J. Tan, M.J. Zaworotko, R.D. Shytle, Improving Lithium Therapeutics by Crystal Engineering of Novel Ionic Cocrystals, Mol. Pharmaceutics. 10 (2013) 4728–4738. doi:10.1021/mp400571a.
[17] A.R. Buist, A.R. Kennedy, Ionic Cocrystals of Pharmaceutical Compounds: Sodium Complexes of Carbamazepine, Cryst. Growth Des. 14 (2014) 6508–6513. doi:10.1021/cg501400n.
[18] J.R.G. Sander, D.-K. Bucar, R.F. Henry, J. Baltrusaitis, G.G.Z. Zhang, L.R. MacGillivray, A Red Zwitterionic Co-Crystal of Acetaminophen and 2,4-Pyridinedicarboxylic Acid, J. Pharm. Sci. 99 (2010) 3676–3683. doi:10.1002/jps.22229.
[19] E.A.J.Y. Prabha, S.S. Kumar, S. Athimoolam, B. Sridhar, Structural, quantum chemical, vibrational and thermal studies of a hydrogen bonded zwitterionic co-crystal (nicotinic acid: pyrogallol), J. Mol. Struct. 1129 (2017) 113–120. doi:10.1016/j.molstruc.2016.09.047.
[20] S.P. Kelley, A. Narita, J.D. Holbrey, K.D. Green, W.M. Reichert, R.D. Rogers, Understanding the Effects of Ionicity in Salts, Solvates, Co-Crystals, Ionic Co-Crystals, and Ionic Liquids, Rather than Nomenclature, Is Critical to Understanding Their Behavior, Cryst. Growth Des. 13 (2013) 965–975. doi:10.1021/cg4000439.
[21] M. Hoffman, J.A. Lindeman, Co-crystals: Commercial Opportunities and Patent Considerations, in: J. Wouters, L. Quéré (Eds.), Pharmaceutical Salts and Co-Crystals, Royal Society of Chemistry, Cambridge, 2011: pp. 318–329.
[22] A. Tilborg, B. Norberg, J. Wouters, Pharmaceutical salts and cocrystals involving amino acids: A brief structural overview of the state-of-art, Eur. J. Med. Chem. 74 (2014) 411–426. doi:10.1016/j.ejmech.2013.11.045.
[23] M.L. Cheney, N. Shan, E.R. Healey, M. Hanna, L. Wojtas, M.J. Zaworotko, V. Sava, S. Song, J.R. Sanchez-Ramos, Effects of Crystal Form on Solubility and Pharmacokinetics: A Crystal Engineering Case Study of Lamotrigine, Cryst. Growth Des. 10 (2010) 394–405. doi:10.1021/cg901010v.
[24] N. Biswas, Solid Forms and Pharmacokinetics, in: J. Wouters, L. Quéré (Eds.), Pharmaceutical Salts and Co-Crystals, Royal Society of Chemistry, Cambridge, 2011: pp. 128–153.
[25] N. Shan, M.L. Perry, D.R. Weyna, M.J. Zaworotko, Impact of pharmaceutical cocrystals: the effects on drug pharmacokinetics, Expert Opin. Drug Metab. Toxicol. 10 (2014) 1255–1271. doi:10.1517/17425255.2014.942281.
[26] P. Gilli, G. Gilli, Noncovalent Interactions in Crystals, in: J.W. Steed, P.A. Gale (Eds.), Supramolecular Chemistry: From Molecules to Nanomaterials, John Wiley & Sons, Ltd, Chichester, UK, 2012: pp. 2829–2867. doi:10.1002/9780470661345.smc110.
[27] C.B. Aakeroy, M.E. Fasulo, J. Desper, Cocrystal or salt: Does it really matter?, Mol. Pharmaceutics. 4 (2007) 317–322. doi:10.1021/mp060126o.
[28] S. Mohamed, D.A. Tocher, S.L. Price, Computational prediction of salt and cocrystal structures-Does a proton position matter?, Int. J. Pharm. 418 (2011) 187–198. doi:10.1016/j.ijpharm.2011.03.063.
[29] D. Luedeker, G. Brunklaus, NMR crystallography of ezetimibe co-crystals, Solid State Nucl. Magn. Reson. 65 (2015) 29–40. doi:10.1016/j.ssnmr.2014.11.002.
[30] D. Luedeker, R. Gossmann, K. Langer, G. Brunklaus, Crystal Engineering of Pharmaceutical Co-crystals: “NMR Crystallography” of Niclosamide Co-crystals, Cryst. Growth Des. 16 (2016) 3087–3100. doi:10.1021/acs.cgd.5b01619.
[31] S. Golob, M. Perry, M. Lusi, M.R. Chierotti, I. Grabnar, L. Lassiani, D. Voinovich, M.J. Zaworotko, Improving Biopharmaceutical Properties of Vinpocetine Through Cocrystallization, J. Pharm. Sci. 105 (2016) 3626–3633. doi:10.1016/j.xphs.2016.09.017.

[32] C.C. da Silva, F.F. Guimaraes, L. Ribeiro, F.T. Martins, Salt or cocrystal of salt? Probing the nature of multicomponent crystal forms with infrared spectroscopy, Spectroc. Acta Pt. A-Molec. Biomolec. Spectr. 167 (2016) 89–95. doi:10.1016/j.saa.2016.05.042.
[33] K. Kawakami, Modification of physicochemical characteristics of active pharmaceutical ingredients and application of supersaturatable dosage forms for improving bioavailability of poorly absorbed drugs, Adv. Drug Deliv. Rev. 64 (2012) 480–495. doi:10.1016/j.addr.2011.10.009.
[34] D. Braga, F. Grepioni, L. Maini, The growing world of crystal forms, Chem. Commun. 46 (2010) 6232–6242. doi:10.1039/c0cc01195a.
[35] G.R. Desiraju, J.J. Vittal, A. Ramanan, Crystal Engineering. A textbook., World Scientific, Singapore, 2011.
[36] G.R. Desiraju, Crystal Engineering: From Molecule to Crystal, J. Am. Chem. Soc. 135 (2013) 9952–9967. doi:10.1021/ja403264c.
[37] A. Mukherjee, Building upon Supramolecular Synthons: Some Aspects of Crystal Engineering, Cryst. Growth Des. 15 (2015) 3076–3085. doi:10.1021/acs.cgd.5b00242.
[38] R. Thipparaboina, D. Kumar, R.B. Chavan, N.R. Shastri, Multidrug co-crystals: towards the development of effective therapeutic hybrids, Drug Discovery Today. 21 (2016) 481–490. doi:10.1016/j.drudis.2016.02.001.
[39] S. Aitipamula, R. Banerjee, A.K. Bansal, K. Biradha, M.L. Cheney, A.R. Choudhury, G.R. Desiraju, A.G. Dikundwar, R. Dubey, N. Duggirala, P.P. Ghogale, S. Ghosh, P.K. Goswami, N.R. Goud, R.R.K.R. Jetti, P. Karpinski, P. Kaushik, D. Kumar, V. Kumar, B. Moulton, A. Mukherjee, G. Mukherjee, A.S. Myerson, V. Puri, A. Ramanan, T. Rajamannar, C.M. Reddy, N. Rodriguez-Hornedo, R.D. Rogers, T.N.G. Row, P. Sanphui, N. Shan, G. Shete, A. Singh, C.C. Sun, J.A. Swift, R. Thaimattam, T.S. Thakur, R.K. Thaper, S.P. Thomas, S. Tothadi, V.R. Vangala, N. Variankaval, P. Vishweshwar, D.R. Weyna, M.J. Zaworotko, Polymorphs, Salts, and Cocrystals: What's in a Name?, Cryst. Growth Des. 12 (2012) 2147–2152. doi:10.1021/cg3002948.
[40] C. Aakeröy, Is there any point in making co-crystals?, Acta Crystallogr., Sect. B: Struct. Sci., Cryst. Eng. Mater. 71 (2015) 387–391. doi:10.1107/S2052520615010872.
[41] A.T.M. Serajuddin, Salt formation to improve drug solubility, Adv. Drug Deliv. Rev. 59 (2007) 603–616. doi:10.1016/j.addr.2007.05.010.
[42] D. Tan, L. Loots, T. Friscic, Towards medicinal mechanochemistry: evolution of milling from pharmaceutical solid form screening to the synthesis of active pharmaceutical ingredients (APIs), Chem. Commun. 52 (2016) 7760–7781. doi:10.1039/c6cc02015a.
[43] C. Saal, A. Becker, Pharmaceutical salts: A summary on doses of salt formers from the Orange Book, Eur. J. Pharm. Sci. 49 (2013) 614–623. doi:10.1016/j.ejps.2013.05.026.
[44] B.M. Collman, J.M. Miller, C. Seadeek, J.A. Stambek, A.C. Blackburn, Comparison of a rational vs. high throughput approach for rapid salt screening and selection, Drug Dev. Ind. Pharm. 39 (2013) 29–38. doi:10.3109/03639045.2012.656272.
[45] A.D. McNaught, A. Wilkinson, eds., IUPAC. Compendium of Chemical Terminology, 2nd ed., Blackwell Scientific Publications, Oxford, 1997.
[46] A.D. Bond, Fundamental Aspects of Salts and Co-crystals, in: J. Wouters, L. Quéré (Eds.), Pharmaceutical Salts and Co-Crystals, Royal Society of Chemistry, Cambridge, 2011: pp. 9–28.
[47] J. Lu, S. Rohani, Preparation and Characterization of Theophylline−Nicotinamide Cocrystal, Org. Process Res. Dev. 13 (2009) 1269–1275. doi:10.1021/op900047r.
[48] C.B. Aakeroey, T.K. Wijethunga, J. Desper, Crystal Engineering of Energetic Materials: Co-crystals of Ethylenedinitramine (EDNA) with Modified Performance and Improved Chemical Stability, Chem.-Eur. J. 21 (2015) 11029–11037. doi:10.1002/chem.201501721.
[49] C.-T. Chen, S. Ghosh, C.M. Reddy, M.J. Buehler, Molecular mechanics of elastic and bendable caffeine co-crystals, Phys. Chem. Chem. Phys. 16 (2014) 13165–13171. doi:10.1039/C3CP55117B.
[50] A. Roberts, L.A. Haighton, A hard look at FDA's review of GRAS notices, Regul. Toxicol. Pharmacol. 79 (2016) S124–S128. doi:10.1016/j.yrtph.2016.06.011.

[51] S.L. Childs, G.P. Stahly, A. Park, The salt-cocrystal continuum: The influence of crystal structure on ionization state, Mol. Pharmaceutics. 4 (2007) 323–338. doi:10.1021/mp0601345.
[52] N.K. Duggirala, M.L. Perry, O. Almarsson, M.J. Zaworotko, Pharmaceutical cocrystals: along the path to improved medicines, Chem. Commun. 52 (2016) 640–655. doi:10.1039/c5cc08216a.
[53] H.G. Brittain, Pharmaceutical cocrystals: The coming wave of new drug substances, J. Pharm. Sci. 102 (2013) 311–317. doi:10.1002/jps.23402.
[54] B.C. Sherman, Solid substances comprising valproic acid and sodium valproate, 6,077,542, 2000.
[55] H.G. Brittain, Stereoselectivity in the Salt-Cocrystal Products formed by Phenylglycinol or Phenylglycine with their Respective Sodium or Hydrochloride Salts, Chirality. 25 (2013) 8–15. doi:10.1002/chir.22103.
[56] P.B. Tarsa, C.S. Towler, G. Woollam, J. Berghausen, The influence of aqueous content in small scale salt screening-Improving hit rate for weakly basic, low solubility drugs, Eur. J. Pharm. Sci. 41 (2010) 23–30. doi:10.1016/j.ejps.2010.05.009.
[57] A. Newman, Specialized Solid Form Screening Techniques, Org. Process Res. Dev. 17 (2013) 457–471. doi:10.1021/op300241f.
[58] L.F. Huang, W.Q. Tong, Impact of solid state properties on developability assessment of drug candidates, Adv. Drug Deliv. Rev. 56 (2004) 321–334. doi:10.1016/j.addr.2003.10.007.
[59] M.J. Bowker, A procedure for salt selection and optimization, in: P.H. Stahl, C.G. Wermuth (Eds.), Handbook of Pharmaceutical Salts, Wiley-VCH, Weinheim, 2002: pp. 161–190.
[60] C.R. Gardner, C.T. Walsh, O. Almarsson, Drugs as materials: Valuing physical form in drug discovery, Nat. Rev. Drug Discov. 3 (2004) 926–934. doi:10.1038/nrd1550.
[61] L. Kumar, A. Amin, A.K. Bansal, An overview of automated systems relevant in pharmaceutical salt screening, Drug Discov. Today. 12 (2007) 1046–1053. doi:10.1016/j.drudis.2007.08.002.
[62] A. Fernández Casares, W.M. Nap, G. Ten Figás, P. Huizenga, R. Groot, M. Hoffmann, An evaluation of salt screening methodologies, J. Pharm. Pharmacol. 67 (2015) 812–822. doi:10.1111/jphp.12377.
[63] N. Qiao, M. Li, W. Schlindwein, N. Malek, A. Davies, G. Trappitt, Pharmaceutical cocrystals: An overview, Int. J. Pharm. 419 (2011) 1–11. doi:10.1016/j.ijpharm.2011.07.037.
[64] G. Kuminek, F. Cao, A.B. de Oliveira da Rocha, S.G. Cardoso, N. Rodriguez-Hornedo, Cocrystals to facilitate delivery of poorly soluble compounds beyond-rule-of-5, Adv. Drug Deliv. Rev. 101 (2016) 143–166. doi:10.1016/j.addr.2016.04.022.
[65] S. Aher, R. Dhumal, K. Mahadik, A. Paradkar, P. York, Ultrasound assisted cocrystallization from solution (USSC) containing a non-congruently soluble cocrystal component pair: Caffeine/maleic acid, Eur. J. Pharm. Sci. 41 (2010) 597–602. doi:10.1016/j.ejps.2010.08.012.
[66] M.D. Eddleston, S. Sivachelvam, W. Jones, Screening for polymorphs of cocrystals: a case study, CrystEngComm. 15 (2013) 175–181. doi:10.1039/c2ce26496j.
[67] L. Padrela, M.A. Rodrigues, S.P. Velaga, A.C. Fernandes, H.A. Matos, E.G. de Azevedo, Screening for pharmaceutical cocrystals using the supercritical fluid enhanced atomization process, J. Supercrit. Fluids. 53 (2010) 156–164. doi:10.1016/j.supflu.2010.01.010.
[68] S.P. Patil, S.R. Modi, A.K. Bansal, Generation of 1:1 Carbamazepine:Nicotinamide cocrystals by spray drying, Eur. J. Pharm. Sci. 62 (2014) 251–257. doi:10.1016/j.ejps.2014.06.001.
[69] V. Sladkova, J. Cibulkova, V. Eigner, A. Sturc, B. Kratochvil, J. Rohlicek, Application and Comparison of Cocrystallization Techniques on Trospium Chloride Cocrystals, Cryst. Growth Des. 14 (2014) 2931–2936. doi:10.1021/cg500226z.
[70] S. Karki, T. Friscic, W. Jones, Control and interconversion of cocrystal stoichiometry in grinding: stepwise mechanism for the formation of a hydrogen-bonded cocrystal, CrystEngComm. 11 (2009) 470–481. doi:10.1039/b812531g.

[71] K. Fucke, S.A. Myz, T.P. Shakhtshneider, E.V. Boldyreva, U.J. Griesser, How good are the crystallisation methods for co-crystals? A comparative study of piroxicam, New J. Chem. 36 (2012) 1969–1977. doi:10.1039/c2nj40093f.
[72] D.R. Weyna, T. Shattock, P. Vishweshwar, M.J. Zaworotko, Synthesis and Structural Characterization of Cocrystals and Pharmaceutical Cocrystals: Mechanochemistry vs Slow Evaporation from Solution, Cryst. Growth Des. 9 (2009) 1106–1123. doi:10.1021/cg800936d.
[73] S.L. James, C.J. Adams, C. Bolm, D. Braga, P. Collier, T. Friscic, F. Grepioni, K.D.M. Harris, G. Hyett, W. Jones, A. Krebs, J. Mack, L. Maini, A.G. Orpen, I.P. Parkin, W.C. Shearouse, J.W. Steed, D.C. Waddell, Mechanochemistry: opportunities for new and cleaner synthesis, Chem. Soc. Rev. 41 (2012) 413–447. doi:10.1039/c1cs15171a.
[74] A.V. Trask, W. Jones, Crystal engineering of organic cocrystals by the solid-state grinding approach, Top. Curr. Chem. 254 (2005) 41–70.
[75] T. Friscic, W. Jones, Recent Advances in Understanding the Mechanism of Cocrystal Formation via Grinding, Cryst. Growth Des. 9 (2009) 1621–1637. doi:10.1021/cg800764n.
[76] D. Braga, L. Maini, F. Grepioni, Mechanochemical preparation of co-crystals, Chem. Soc. Rev. 42 (2013) 7638–7648. doi:10.1039/c3cs60014a.
[77] D.J. Berry, C.C. Seaton, W. Clegg, R.W. Harrington, S.J. Coles, P.N. Horton, M.B. Hursthouse, R. Storey, W. Jones, T. Friscic, N. Blagden, Applying hot-stage microscopy to co-crystal screening: A study of nicotinamide with seven active pharmaceutical ingredients, Cryst. Growth Des. 8 (2008) 1697–1712. doi:10.1021/cg800035w.
[78] D. Braga, F. Grepioni, G.I. Lampronti, L. Maini, K. Rubini, A. Turrina, F. Zorzi, Crystal form selectivity by humidity control: the case of the ionic co-crystals of nicotinamide and CaCl2, CrystEngComm. 16 (2014) 7452–7458. doi:10.1039/c4ce00464g.
[79] W. Beckmann, Seeding the desired polymorph: Background, possibilities, limitations, and case studies, Org. Process Res. Dev. 4 (2000) 372–383. doi:10.1021/op0000778.
[80] D. Braga, F. Grepioni, L. Maini, M. Polito, K. Rubini, M.R. Chierotti, R. Gobetto, Hetero-Seeding and Solid Mixture to Obtain New Crystalline Forms, Chem.-Eur. J. 15 (2009) 1508–1515. doi:10.1002/chem.200800381.
[81] T.L. Threlfall, R.W. De'Ath, S.J. Coles, Metastable Zone Widths, Conformational Multiplicity, and Seeding, Org. Process Res. Dev. 17 (2013) 578–584. doi:10.1021/op3003486.
[82] K.D.M. Harris, E.Y. Cheung, How to determine structures when single crystals cannot be grown: opportunities for structure determination of molecular materials using powder diffraction data, Chem. Soc. Rev. 33 (2004) 526–538. doi:10.1039/b409059b.
[83] K. Shankland, M.J. Spillman, E.A. Kabova, D.S. Edgeley, N. Shankland, The principles underlying the use of powder diffraction data in solving pharmaceutical crystal structures, Acta Crystallogr. Sect. C-Cryst. Struct. Commun. 69 (2013) 1251–1259. doi:10.1107/S0108270113028643.
[84] S.H. Lapidus, P.W. Stephens, K.K. Arora, T.R. Shattock, M.J. Zaworotko, A Comparison of Cocrystal Structure Solutions from Powder and Single Crystal Techniques, Cryst. Growth Des. 10 (2010) 4630–4637. doi:10.1021/cg1009237.
[85] Y.G. Andreev, G.S. MacGlashan, P.G. Bruce, Ab initio solution of a complex crystal structure from powder-diffraction data using simulated-annealing method and a high degree of molecular flexibility, Phys. Rev. B. 55 (1997) 12011–12017. doi:10.1103/PhysRevB.55.12011.
[86] V. Favre-Nicolin, R. Cerny, FOX, "free objects for crystallography": a modular approach to ab initio structure determination from powder diffraction, J. Appl. Crystallogr. 35 (2002) 734–743. doi:10.1107/S0021889802015236.
[87] S.Y. Chong, M. Tremayne, Combined optimization using cultural and differential evolution: application to crystal structure solution from powder diffraction data, Chem. Commun. (2006) 4078–4080. doi:10.1039/b609138e.

[88] A. Altomare, C. Cuocci, C. Giacovazzo, A. Moliterni, R. Rizzi, N. Corriero, A. Falcicchio, EXPO2013: a kit of tools for phasing crystal structures from powder data, J. Appl. Crystallogr. 46 (2013) 1231–1235. doi:10.1107/S0021889813013113.
[89] L. Palatinus, G. Chapuis, SUPERFLIP - a computer program for the solution of crystal structures by charge flipping in arbitrary dimensions, J. Appl. Crystallogr. 40 (2007) 786–790. doi:10.1107/S0021889807029238.
[90] X. Filip, G. Borodi, C. Filip, Testing the limits of sensitivity in a solid-state structural investigation by combined X-ray powder diffraction, solid-state NMR, and molecular modelling, Phys. Chem. Chem. Phys. 13 (2011) 17978–17986. doi:10.1039/c1cp21878f.
[91] G.K. Lim, K. Fujii, K.D.M. Harris, D.C. Apperley, Structure Determination from Powder X-ray Diffraction Data of a New Polymorph of a High-Density Organic Hydrate Material, with an Assessment of Hydrogen-Bond Disorder by Rietveld Refinement, Cryst. Growth Des. 11 (2011) 5192–5199. doi:10.1021/cg201230k.
[92] S.L. Bekoe, D. Urmann, A. Lakatos, C. Glaubitz, M.U. Schmidt, Nimustine hydrochloride: the first crystal structure determination of a 2-chloroethyl-N-nitrosourea hydrochloride derivative by X-ray powder diffraction and solid-state NMR, Acta Crystallogr. Sect. C-Cryst. Struct. Commun. 68 (2012) O144–O148. doi:10.1107/S0108270112005252.
[93] D.V. Dudenko, P.A. Williams, C.E. Hughes, O.N. Antzutkin, S.P. Velaga, S.P. Brown, K.D.M. Harris, Exploiting the Synergy of Powder X-ray Diffraction and Solid-State NMR Spectroscopy in Structure Determination of Organic Molecular Solids, J. Phys. Chem. C. 117 (2013) 12258–12265. doi:10.1021/jp4041106.
[94] D. Braga, L. Chelazzi, F. Grepioni, E. Dichiarante, M.R. Chierotti, R. Gobetto, Molecular Salts of Anesthetic Lidocaine with Dicarboxylic Acids: Solid-State Properties and a Combined Structural and Spectroscopic Study, Cryst. Growth Des. 13 (2013) 2564–2572. doi:10.1021/cg400331h.
[95] R.K. Harris, NMR crystallography: the use of chemical shifts, Solid State Sci. 6 (2004) 1025–1037. doi:10.1016/j.solidstatesciences.2004.03.040.
[96] M.U. Schmidt, J. Bruening, J. Glinnemann, M.W. Huetzler, P. Moerschel, S.N. Ivashevskaya, J. van de Streek, D. Braga, L. Maini, M.R. Chierotti, R. Gobetto, The Thermodynamically Stable Form of Solid Barbituric Acid: The Enol Tautomer, Angew. Chem., Int. Edit. 50 (2011) 7924–7926. doi:10.1002/anie.201101040.
[97] F.G. Vogt, J.S. Clawson, M. Strohmeier, A.J. Edwards, T.N. Pham, S.A. Watson, Solid-State NMR Analysis of Organic Cocrystals and Complexes, Cryst. Growth Des. 9 (2009) 921–937. doi:10.1021/cg8007014.
[98] K. Maruyoshi, D. Iuga, O.N. Antzutkin, A. Alhalaweh, S.P. Velagad, S.P. Brown, Identifying the intermolecular hydrogen-bonding supramolecular synthons in an indomethacin-nicotinamide cocrystal by solid-state NMR, Chem. Commun. 48 (2012) 10844–10846. doi:10.1039/c2cc36094b.
[99] T. Kojima, S. Tsutsumi, K. Yamamoto, Y. Ikeda, T. Moriwaki, High-throughput cocrystal slurry screening by use of in situ Raman microscopy and multi-well plate, Int. J. Pharm. 399 (2010) 52–59. doi:10.1016/j.ijpharm.2010.07.055.
[100] A. Mukherjee, S. Tothadi, S. Chakraborty, S. Ganguly, G.R. Desiraju, Synthon identification in co-crystals and polymorphs with IR spectroscopy. Primary amides as a case study, CrystEngComm. 15 (2013) 4640–4654. doi:10.1039/c3ce40286j.
[101] J.C. Burley, A. Alkhalil, M. Bloomfield, P. Matousek, Transmission Raman spectroscopy for quality control in model cocrystal tablets, Analyst. 137 (2012) 3052–3057. doi:10.1039/c2an35216h.
[102] D. Giron, Applications of thermal analysis and coupled techniques in pharmaceutical industry, J. Therm. Anal. 68 (2002) 335–357. doi:10.1023/A:1016015113795.
[103] D.Q.M. Craig, M. Reading, eds., Thermal analysis of Pharmaceuticals, CRC Press, Boca Raton, FL, 2006.

[104] I.M. Vitez, A.W. Newman, M. Davidovich, C. Kiesnowski, The evolution of hot-stage microscopy to aid solid-state characterizations of pharmaceutical solids, Thermochim. Acta. 324 (1998) 187–196. doi:10.1016/S0040-6031(98)00535-8.
[105] T. Ueto, N. Takata, N. Muroyama, A. Nedu, A. Sasaki, S. Tanida, K. Terada, Polymorphs and a Hydrate of Furosemide-Nicotinamide 1:1 Cocrystal, Cryst. Growth Des. 12 (2012) 485–494. doi:10.1021/cg2013232.
[106] J. Li, S.A. Bourne, M.M. de Villiers, A.M. Crider, M.R. Caira, Polymorphism of the Antitubercular Isoxyl, Cryst. Growth Des. 11 (2011) 4950–4957. doi:10.1021/cg200860p.
[107] J.S. Stevens, L.K. Newton, C. Jaye, C.A. Muryn, D.A. Fischer, S.L.M. Schroeder, Proton Transfer, Hydrogen Bonding, and Disorder: Nitrogen Near-Edge X-ray Absorption Fine Structure and X-ray Photoelectron Spectroscopy of Bipyridine-Acid Salts and Co-crystals, Cryst. Growth Des. 15 (2015) 1776–1783. doi:10.1021/cg5018278.
[108] E.P.J. Parrott, J.A. Zeitler, T. Friscic, M. Pepper, W. Jones, G.M. Day, L.F. Gladden, Testing the Sensitivity of Terahertz Spectroscopy to Changes in Molecular and Supramolecular Structure: A Study of Structurally Similar Cocrystals, Cryst. Growth Des. 9 (2009) 1452–1460. doi:10.1021/cg8008893.
[109] G.A. Jeffrey, An Introduction to Hydrogen Bonding., Oxford University Press, New York, 1997.
[110] R. Taylor, O. Kennard, Hydrogen-Bond Geometry in Organic-Crystals, Acc. Chem. Res. 17 (1984) 320–326. doi:10.1021/ar00105a004.
[111] C.L. Nygren, C.C. Wilson, J.F.C. Turner, Electron and nuclear positions in the short hydrogen bond in urotropine-N-oxide-formic acid, J. Phys. Chem. A. 109 (2005) 1911–1919. doi:10.1021/jp047187r.
[112] D. Wiechert, D. Mootz, Molecular beside ionic: Crystal structures of a 1/1 and a 1/4 adduct of pyridine and formic acid, Angew. Chem., Int. Edit. 38 (1999) 1974–1976. doi:10.1002/(SICI)1521-3773(19990712)38:13/14<1974::AID-ANIE1974>3.0.CO;2-F.
[113] T. Steiner, I. Majerz, C.C. Wilson, First O-H-N hydrogen fond with a centered proton obtained by thermally induced proton migration, Angew. Chem., Int. Edit. 40 (2001) 2651–2654. doi:10.1002/1521-3773(20010716)40:14<2651::AID-ANIE2651>3.0.CO;2-2.
[114] L.H. Thomas, N. Blagden, M.J. Gutmann, A.A. Kallay, A. Parkin, C.C. Seaton, C.C. Wilson, Tuning Proton Behavior in a Ternary Molecular Complex, Cryst. Growth Des. 10 (2010) 2770–2774. doi:10.1021/cg100315u.
[115] H. Yamashita, Y. Hirakura, M. Yuda, K. Terada, Coformer Screening Using Thermal Analysis Based on Binary Phase Diagrams, Pharm. Res. 31 (2014) 1946–1957. doi:10.1007/s11095-014-1296-4.
[116] Guidance for Industry. Regulatory classification of pharmaceutical co-crystals, (2013). https://www.fda.gov/downloads/Drugs/Guidances/UCM281764.pdf (accessed February 22, 2017).
[117] N. Schultheiss, A. Newman, Pharmaceutical Cocrystals and Their Physicochemical Properties, Cryst. Growth Des. 9 (2009) 2950–2967. doi:10.1021/cg900129f.
[118] D.P. McNamara, S.L. Childs, J. Giordano, A. Iarriccio, J. Cassidy, M.S. Shet, R. Mannion, E. O'Donnell, A. Park, Use of a glutaric acid cocrystal to improve oral bioavailability of a low solubility API, Pharm. Res. 23 (2006) 1888–1897. doi:10.1007/s11095-006-9032-3.
[119] C.B. Aakeroy, I. Hussain, J. Desper, 2-Acetaminopyridine: A highly effective cocrystallizing agent, Cryst. Growth Des. 6 (2006) 474–480. doi:10.1021/cg050391z.
[120] C.B. Aakeroey, A. Rajbanshi, Z.J. Li, J. Desper, Mapping out the synthetic landscape for re-crystallization, co-crystallization and salt formation, CrystEngComm. 12 (2010) 4231–4239. doi:10.1039/c0ce00052c.
[121] C.C.P. da Silva, R. de Oliveira, J.C. Tenorio, S.B. Honorato, A.P. Ayala, J. Ellena, The Continuum in 5-Fluorocytosine. Toward Salt Formation, Cryst. Growth Des. 13 (2013) 4315–4322. doi:10.1021/cg400662n.

[122] R.M. Silverstein, F.X. Webster, D.J. Kiemle, Infrared Spectrometry, in: Spectrometric Identification of Organic Compounds, 7th ed., John Wiley & Sons, Inc., New York, 2005: pp. 72–126.
[123] S. Chakraborty, S. Ganguly, G.R. Desiraju, Synthon transferability probed with IR spectroscopy: cytosine salts as models for salts of lamivudine, CrystEngComm. 16 (2014) 4732–4741. doi:10.1039/c3ce42156b.
[124] A.C. Doriguetto, F.T. Martins, J. Ellena, R. Salloum, M.H. dos Santos, M.E.C. Moreira, J.M. Schneedorf, T.J. Nagem, 2,2',4-trihydroxybenzophenone: Crystal structure, and anti-inflammatory and antioxidant activities, Chem. Biodivers. 4 (2007) 488–499. doi:10.1002/cbdv.200790041.
[125] F.T. Martins, F.F. Guimaraes, S.B. Honorato, A.P. Ayala, J. Ellena, Vibrational and thermal analyses of multicomponent crystal forms of the anti-HIV drugs lamivudine and zalcitabine, J. Pharm. Biomed. Anal. 110 (2015) 76–82. doi:10.1016/j.jpba.2015.03.004.
[126] J. Lu, Y.-P. Li, J. Wang, Z. Li, S. Rohani, C.-B. Ching, Pharmaceutical cocrystals: a comparison of sulfamerazine with sulfamethazine, J. Cryst. Growth. 335 (2011) 110–114. doi:10.1016/j.jcrysgro.2011.09.032.
[127] G. Socrates, ed., Infrared and Raman Characteristic Group Frequencies-Tables and Charts, 3rd ed., John Wiley & Sons, Ltd, Chichester, UK, 2001.
[128] A.E. Aliev, K.D.M. Harris, Probing Hydrogen Bonding in Solids Using Solid State NMR Spectroscopy, in: D.M.P. Mingos (Ed.), Supramolecular Assembly via Hydrogen Bonds I, Springer Berlin Heidelberg, 2004: pp. 1–53. doi:10.1007/b14136.
[129] T. Steiner, The hydrogen bond in the solid state, Angew. Chem., Int. Edit. 41 (2002) 48–76. doi:10.1002/1521-3773(20020104)41:1<48::AID-ANIE48>3.0.CO;2-U.
[130] D. Bugay, Solid-State Nuclear-Magnetic-Resonance Spectroscopy - Theory and Pharmaceutical Applications, Pharm. Res. 10 (1993) 317–327. doi:10.1023/A:1018967717781.
[131] M.R. Chierotti, R. Gobetto, Solid-state NMR studies of weak interactions in supramolecular systems, Chem. Commun. (2008) 1621–1634. doi:10.1039/B711551B.
[132] M.R. Chierotti, R. Gobetto, NMR crystallography: the use of dipolar interactions in polymorph and co-crystal investigation, CrystEngComm. 15 (2013) 8599–8612. doi:10.1039/c3ce41026a.
[133] Y. Nishiyama, Fast magic-angle sample spinning solid-state NMR at 60–100 kHz for natural abundance samples, Solid State Nucl. Magn. Reson. 78 (2016) 24–36. doi:10.1016/j.ssnmr.2016.06.002.
[134] S.P. Brown, Applications of high-resolution 1H solid-state NMR, Solid State Nucl. Magn. Reson. 41 (2012) 1–27. doi:10.1016/j.ssnmr.2011.11.006.
[135] D. Braga, L. Maini, G. de Sanctis, K. Rubini, F. Grepioni, M.R. Chierotti, R. Gobetto, Mechanochemical preparation of hydrogen-bonded adducts between the diamine 1,4-diazabicyclo [2.2.2] octane and dicarboxylic acids of variable chain length: An x-ray diffraction and solid-state NMR study, Chem.-Eur. J. 9 (2003) 5538–5548. doi:10.1002/chem.200304940.
[136] A. Bacchi, G. Cantoni, M.R. Chierotti, A. Girlando, R. Gobetto, G. Lapadula, P. Pelagatti, A. Sironi, M. Zecchini, Water vapour uptake and extrusion by a crystalline metallorganic solid based on half-sandwich Ru(II) building-blocks, CrystEngComm. 13 (2011) 4365–4375. doi:10.1039/c0ce00816h.
[137] M.R. Chierotti, R. Gobetto, C. Nervi, A. Bacchi, P. Pelagatti, V. Colombo, A. Sironi, Probing Hydrogen Bond Networks in Half-Sandwich Ru(II) Building Blocks by a Combined H-1 DQ CRAMPS Solid-State NMR, XRPD, and DFT Approach, Inorg. Chem. 53 (2014) 139–146. doi:10.1021/ic401762z.
[138] A. Kotar, M. Kotar, P. Sketa, J. Plavec, Potential of Solid-state NMR and SEM in Characterization of Tablets of Ibuprofen, Curr. Pharm. Anal. 11 (2015) 124–130.

[139] A.T. Vasconcelos, C.C. da Silva, L.H. Keng Queiroz Junior, M.J. Santana, V.S. Ferreira, F.T. Martins, Lamivudine as a Nucleoside Template To Engineer DNA-Like Double-Stranded Helices in Crystals, Cryst. Growth Des. 14 (2014) 4691–4702. doi:10.1021/cg500786m.
[140] O.D. Putra, T. Yoshida, D. Umeda, K. Higashi, H. Uekusa, E. Yonemochi, Crystal Structure Determination of Dimenhydrinate after More than 60 Years: Solving Salt-Cocrystal Ambiguity via Solid-State Characterizations and Solubility Study, Cryst. Growth Des. 16 (2016) 5223–5229. doi:10.1021/acs.cgd.6b00771.
[141] A. Naito, S. Ganapathy, K. Akasaka, C. Mcdowell, Chemical Shielding Tensor and C-13-N-14 Dipolar Splitting in Single-Crystals of L-Alanine, J. Chem. Phys. 74 (1981) 3190–3197. doi:10.1063/1.441513.
[142] R. Haberkorn, R. Stark, H. Vanwilligen, R. Griffin, Determination of Bond Distances and Bond Angles by Solid-State Nuclear Magnetic-Resonance - C-13 and N-14 Nmr-Study of Glycine, J. Am. Chem. Soc. 103 (1981) 2534–2539. doi:10.1021/ja00400a008.
[143] N. Janes, S. Ganapathy, E. Oldfield, C-13 Chemical Shielding Tensors in L-Threonine, J. Magn. Reson. 54 (1983) 111–121. doi:10.1016/0022-2364(83)90150-6.
[144] R. Griffin, A. Pines, S. Pausak, J. Waugh, C-13 Chemical Shielding in Oxalic-Acid, Oxalic-Acid Dihydrate, and Diammonium Oxalate, J. Chem. Phys. 63 (1975) 1267–1271. doi:10.1063/1.431418.
[145] W.S. Veeman, Carbon-13 chemical shift anisotropy, Prog. Nucl. Magn. Reson. Spectrosc. 16 (1984) 193–235. doi:10.1016/0079-6565(84)80006-0.
[146] D.H. Brouwer, J.A. Ripmeester, Symmetry-based recoupling of proton chemical shift anisotropies in ultrahigh-field solid-state NMR, J. Magn. Reson. 185 (2007) 173–178. doi:10.1016/j.jmr.2006.12.003.
[147] M. Carravetta, M. Eden, X. Zhao, A. Brinkmann, M.H. Levitt, Symmetry principles for the design of radiofrequency pulse sequences in the nuclear magnetic resonance of rotating solids, Chem. Phys. Lett. 321 (2000) 205–215. doi:10.1016/S0009-2614(00)00340-7.
[148] M.H. Levitt, Symmetry in the design of NMR multiple-pulse sequences, J. Chem. Phys. 128 (2008) 52205. doi:10.1063/1.2831927.
[149] L. Duma, D. Abergel, P. Tekely, G. Bodenhausen, Proton chemical shift anisotropy measurements of hydrogen-bonded functional groups by fast magic-angle spinning solid-state NMR spectroscopy, Chem. Commun. (2008) 2361–2363. doi:10.1039/b801154k.
[150] E.R. Andrew, A. Bradbury, R.G. Eades, V.T. Wynn, Nuclear cross-relaxation induced by specimen rotation, Phys. Lett. 4 (1963) 99–100. doi:10.1016/0031-9163(63)90123-9.
[151] T. Oas, R. Griffin, M. Levitt, Rotary Resonance Recoupling of Dipolar Interactions in Solid-State Nuclear Magnetic-Resonance Spectroscopy, J. Chem. Phys. 89 (1988) 692–695. doi:10.1063/1.455191.
[152] Z.H. Gan, D.M. Grant, R.R. Ernst, NMR chemical shift anisotropy measurements by RF driven rotary resonance, Chem. Phys. Lett. 254 (1996) 349–357. doi:10.1016/0009-2614(96)00268-0.
[153] C. Rohlfing, L. Allen, R. Ditchfield, Proton Chemical-Shift Tensors in Hydrogen-Bonded Dimers of Rcooh and Roh, J. Chem. Phys. 79 (1983) 4958–4966. doi:10.1063/1.445589.
[154] M. Kibalchenko, D. Lee, L. Shao, M.C. Payne, J.J. Titman, J.R. Yates, Distinguishing hydrogen bonding networks in alpha-D-galactose using NMR experiments and first principles calculations, Chem. Phys. Lett. 498 (2010) 270–276. doi:10.1016/j.cplett.2010.08.077.
[155] G. Wu, C.J. Freure, E. Verdurand, Proton chemical shift tensors and hydrogen bond geometry: A (1)H-(2)H dipolar NMR study of the water molecule in crystalline hydrates, J. Am. Chem. Soc. 120 (1998) 13187–13193. doi:10.1021/ja983126t.
[156] J. Herzfeld, A. Berger, Sideband Intensities in Nmr-Spectra of Samples Spinning at the Magic Angle, J. Chem. Phys. 73 (1980) 6021–6030. doi:10.1063/1.440136.

[157] J. Viger-Gravel, I. Korobkov, D.L. Bryce, Multinuclear Solid-State Magnetic Resonance and X-ray Diffraction Study of Some Thiocyanate and Selenocyanate Complexes Exhibiting Halogen Bonding, Cryst. Growth Des. 11 (2011) 4984–4995. doi:10.1021/cg200889y.
[158] S.M. De Paul, K. Saalwachter, R. Graf, H.W. Spiess, Sideband patterns from rotor-encoded longitudinal magnetization in MAS recoupling experiments, J. Magn. Reson. 146 (2000) 140–156. doi:10.1006/jmre.2000.2119.
[159] Y.F. Wei, D.K. Lee, A.E. McDermott, A. Ramamoorthy, A 2D MAS solid-state NMR method to recover the amplified heteronuclear dipolar and chemical shift anisotropic interactions, J. Magn. Reson. 158 (2002) 23–35. doi:10.1016/S1090-7807(02)00056-3.
[160] O. Antzutkin, S. Shekar, M. Levitt, 2-Dimensional Side-Band Separation in Magic-Angle-Spinning Nmr, J. Magn. Reson. Ser. A. 115 (1995) 7–19. doi:10.1006/jmra.1995.1142.
[161] O.N. Antzutkin, Y.K. Lee, M.H. Levitt, C-13 and N-15 chemical shift anisotropy of ampicillin and penicillin-V studied by 2D-PASS and CP/MAS NMR, J. Magn. Reson. 135 (1998) 144–155. doi:10.1006/jmre.1998.1576.
[162] S.N. Smirnov, N.S. Golubev, G.S. Denisov, H. Benedict, P. SchahMohammedi, H.H. Limbach, Hydrogen deuterium isotope effects on the NMR chemical shifts and geometries of intermolecular low-barrier hydrogen-bonded complexes, J. Am. Chem. Soc. 118 (1996) 4094–4101. doi:10.1021/ja953445+.
[163] R. Gobetto, C. Nervi, E. Valfre, M.R. Chierotti, D. Braga, L. Maini, F. Grepioni, R.K. Harris, P.Y. Ghi, H-1 MAS, N-15 CPMAS, and DFT investigation of hydrogen-bonded supramolecular adducts between the diamine 1,4-diazabicyclo-[2.2.2]octane and dicarboxylic acids of variable chain length, Chem. Mat. 17 (2005) 1457–1466. doi:10.1021/cm049063x.
[164] R. Gobetto, C. Nervi, M.R. Chierotti, D. Braga, L. Maini, F. Grepioni, R.K. Harris, P. Hodgkinson, Hydrogen Bonding and Dynamic Behaviour in Crystals and Polymorphs of Dicarboxylic–Diamine Adducts: A Comparison between NMR Parameters and X-ray Diffraction Studies, Chem. - Eur. J. 11 (2005) 7461–7471. doi:10.1002/chem.200500616.
[165] C. Foces-Foces, A. Echevarria, N. Jagerovic, I. Alkorta, J. Elguero, U. Langer, O. Klein, M. Minguet-Bonvehi, H.H. Limbach, A solid-state NMR, X-ray diffraction, and ab initio computational study of hydrogen-bond structure and dynamics of pyrazole-4-carboxylic acid chains, J. Am. Chem. Soc. 123 (2001) 7898–7906. doi:10.1021/ja002688l.
[166] F. Marchetti, J. Palmucci, C. Pettinari, R. Pettinari, F. Condello, S. Ferraro, M. Marangoni, A. Crispini, S. Scuri, I. Grappasonni, M. Cocchioni, M. Nabissi, M.R. Chierotti, R. Gobetto, Novel Composite Plastics Containing Silver(I) Acylpyrazolonato Additives Display Potent Antimicrobial Activity by Contact, Chem.-Eur. J. 21 (2015) 836–850. doi:10.1002/chem.201404812.
[167] R. Pettinari, C. Pettinari, F. Marchetti, R. Gobetto, C. Nervi, M.R. Chierotti, E.J. Chan, B.W. Skelton, A.H. White, Solid-State N-15 CPMAS NMR and Computational Analysis of Ligand Hapticity in Rhodium(eta-diene) Poly(pyrazolyl)borate Complexes, Inorg. Chem. 49 (2010) 11205–11215. doi:10.1021/ic101830e.
[168] Z.J. Li, Y. Abramov, J. Bordner, J. Leonard, A. Medek, A.V. Trask, Solid-state acid-base interactions in complexes of heterocyclic bases with dicarboxylic acids: Crystallography, hydrogen bond analysis, and N-15 NMR spectroscopy, J. Am. Chem. Soc. 128 (2006) 8199–8210. doi:10.1021/ja0541332.
[169] B. Osmialowski, E. Kolehmainen, K. Ejsmont, S. Ikonen, A. Valkonen, K. Rissanen, Nonappa, Association of 2-acylaminopyridines and benzoic acids. Steric and electronic substituent effect studied by XRD, solution and solid-state NMR and calculations, J. Mol. Struct. 1054 (2013) 157–163. doi:10.1016/j.molstruc.2013.09.047.
[170] Y. Song, X. Yang, X. Chen, H. Nie, S. Byrn, J.W. Lubach, Investigation of Drug-Excipient Interactions in Lapatinib Amorphous Solid Dispersions Using Solid-State NMR Spectroscopy, Mol. Pharmaceutics. 12 (2015) 857–866. doi:10.1021/mp500692a.

[171] P. Bencsath, L. Debreczeni, L. Takacs, Effect of Ethyl Apovincaminate on Cerebral-Circulation of Dogs Under Normal Conditions and in Arterial Hypoxia, Arzneimittelforschung. 26 (1976) 1920–1923.
[172] D. Hasa, B. Perissutti, S. Dall'Acqua, M.R. Chierotti, R. Gobetto, I. Grabnar, C. Cepek, D. Voinovich, Rationale of using Vinca minor Linne dry extract phytocomplex as a vincamine's oral bioavailability enhancer, Eur. J. Pharm. Biopharm. 84 (2013) 138–144. doi:10.1016/j.ejpb.2012.11.025.
[173] D. Hasa, B. Perissutti, M.R. Chierotti, R. Gobetto, I. Grabnar, A. Bonifacio, S. Dall'Acqua, S. Invernizzi, D. Voinovich, Mechanochemically induced disordered structures of vincamine: The different mediation of two cross-linked polymers, Int. J. Pharm. 436 (2012) 41–57. doi:10.1016/j.ijpharm.2012.06.024.
[174] D. Hasa, B. Perissutti, M. Grassi, M.R. Chierotti, R. Gobetto, V. Ferrario, D. Lenaz, D. Voinovich, Mechanochemical activation of vincamine mediated by linear polymers: Assessment of some "critical" steps, Eur. J. Pharm. Sci. 50 (2013) 56–68. doi:10.1016/j.ejps.2013.03.003.
[175] D. Hasa, D. Voinovich, B. Perissutti, M. Grassi, A. Bonifacio, V. Sergo, C. Cepek, M.R. Chierotti, R. Gobetto, S. Dall'Acqua, S. Invernizzi, Enhanced Oral Bioavailability of Vinpocetine Through Mechanochemical Salt Formation: Physico-Chemical Characterization and In Vivo Studies, Pharm. Res. 28 (2011) 1870–1883. doi:10.1007/s11095-011-0415-8.
[176] D.C. Apperley, P.A. Basford, C.I. Dallman, R.K. Harris, M. Kinns, P.V. Marshall, A.G. Swanson, Nuclear magnetic resonance investigation of the interaction of water vapor with sildenafil citrate in the solid state, J. Pharm. Sci. 94 (2005) 516–523. doi:10.1002/jps.20271.
[177] A. Peresypkin, N. Variankaval, R. Ferlita, R. Wenslow, J. Smitrovich, K. Thompson, J. Murry, L. Crocker, D. Mathre, J. Wang, P. Harmon, M. Ellison, S. Song, A. Makarov, R. Helmy, Discovery of a stable molecular complex of an API with HCl: A long journey to a conventional salt, J. Pharm. Sci. 97 (2008) 3721–3726. doi:10.1002/jps.21264.
[178] M. Sardo, S.M. Santos, A.A. Babaryk, C. Lopez, I. Alkorta, J. Elguero, R.M. Claramunt, L. Mafra, Diazole-based powdered cocrystal featuring a helical hydrogen-bonded network: Structure determination from PXRD, solid-state NMR and computer modeling, Solid State Nucl. Magn. Reson. 65 (2015) 49–63. doi:10.1016/j.ssnmr.2014.12.005.
[179] A. Lesage, P. Charmont, S. Steuernagel, L. Emsley, Complete resonance assignment of a natural abundance solid peptide by through-bond heteronuclear correlation solid-state NMR, J. Am. Chem. Soc. 122 (2000) 9739–9744. doi:10.1021/ja0018320.
[180] M.K. Pandey, J.-P. Amoureux, T. Asakura, Y. Nishiyama, Sensitivity enhanced N-14/N-14 correlations to probe inter-beta-sheet interactions using fast magic angle spinning solid-state NMR in biological solids, Phys. Chem. Chem. Phys. 18 (2016) 22583–22589. doi:10.1039/c6cp03848d.
[181] S.D. Gumbert, M. Koerbitzer, E. Alig, M.U. Schmidt, M.R. Chierotti, R. Gobetto, X. Li, J. van de Streek, Crystal structure and tautomerism of Pigment Yellow 138 determined by X-ray powder diffraction and solid-state NMR, Dyes Pigm. 131 (2016) 364–372. doi:10.1016/j.dyepig.2016.03.035.
[182] M. Shen, J. Trébosc, O. Lafon, Z. Gan, F. Pourpoint, B. Hu, Q. Chen, J.-P. Amoureux, Solid-state NMR indirect detection of nuclei experiencing large anisotropic interactions using spinning sideband-selective pulses, Solid State Nucl. Magn. Reson. 72 (2015) 104–117. doi:10.1016/j.ssnmr.2015.09.003.
[183] G.N.M. Reddy, D.S. Cook, D. Iuga, R.I. Walton, A. Marsh, S.P. Brown, An NMR crystallography study of the hemihydrate of 2′, 3′-O-isopropylidineguanosine, Solid State Nucl. Magn. Reson. 65 (2015) 41–48. doi:10.1016/j.ssnmr.2015.01.001.
[184] Y. Nishiyama, Y. Endo, T. Nemoto, H. Utsumi, K. Yamauchi, K. Hioka, T. Asakura, Very fast magic angle spinning H-1-N-14 2D solid-state NMR: Sub-micro-liter sample data collection in a few minutes, J. Magn. Reson. 208 (2011) 44–48. doi:10.1016/j.jmr.2010.10.001.

[185] A.S. Tatton, T.N. Pham, F.G. Vogt, D. Iuga, A.J. Edwards, S.P. Brown, Probing intermolecular interactions and nitrogen protonation in pharmaceuticals by novel N-15-edited and 2D N-14-H-1 solid-state NMR, CrystEngComm. 14 (2012) 2654–2659. doi:10.1039/c2ce06547a.
[186] S.L. Veinberg, K.E. Johnston, M.J. Jaroszewicz, B.M. Kispal, C.R. Mireault, T. Kobayashi, M. Pruski, R.W. Schurko, Natural abundance 14N and 15N solid-state NMR of pharmaceuticals and their polymorphs, Phys. Chem. Chem. Phys. 18 (2016) 17713–17730. doi:10.1039/C6CP02855A.
[187] P. Cerreia Vioglio, L. Catalano, V. Vasylyeva, C. Nervi, M.R. Chierotti, G. Resnati, R. Gobetto, P. Metrangolo, Natural Abundance 15N and 13C Solid-State NMR Chemical Shifts: High Sensitivity Probes of the Halogen Bond Geometry, Chem. – Eur. J. 22 (2016) 16819–16828. doi:10.1002/chem.201603392.
[188] P. Cerreia Vioglio, M.R. Chierotti, R. Gobetto, Solid-state nuclear magnetic resonance as a tool for investigating the halogen bond, CrystEngComm. 18 (2016) 9173–9184. doi:10.1039/c6ce02219g.
[189] M.S. Solum, K.L. Altmann, M. Strohmeier, D.A. Berges, Y.L. Zhang, J.C. Facelli, R.J. Pugmire, D.M. Grant, N-15 chemical shift principal values in nitrogen heterocycles, J. Am. Chem. Soc. 119 (1997) 9804–9809. doi:10.1021/ja964135+.
[190] D. Schweitzer, H.W. Spiess, Nitrogen-15 NMR of pyridine in high magnetic: Fields, J. Magn. Reson. 15 (1974) 529–539. doi:10.1016/0022-2364(74)90155-3.
[191] R.W. Schurko, R.E. Wasylishen, Nitrogen-15 NMR study of solid cobaloximes containing N-15-labeled pyridine and aniline, J. Phys. Chem. A. 104 (2000) 3410–3420. doi:10.1021/jp994254m.
[192] P. Lorente, I.G. Shenderovich, N.S. Golubev, G.S. Denisov, G. Buntkowsky, H.H. Limbach, H-1/N-15 NMR chemical shielding, dipolar N-15, H-2 coupling and hydrogen bond geometry correlations in a novel series of hydrogen-bonded acid-base complexes of collidine with carboxylic acids, Magn. Reson. Chem. 39 (2001) S18–S29. doi:10.1002/mrc.946.
[193] C.J. Pickard, F. Mauri, All-electron magnetic response with pseudopotentials: NMR chemical shifts, Phys. Rev. B. 63 (2001) 245101. doi:10.1103/PhysRevB.63.245101.
[194] J.R. Yates, C.J. Pickard, F. Mauri, Calculation of NMR chemical shifts for extended systems using ultrasoft pseudopotentials, Phys. Rev. B. 76 (2007) 24401. doi:10.1103/PhysRevB.76.024401.
[195] M. Khan, V. Enkelmann, G. Brunklaus, Heterosynthon mediated tailored synthesis of pharmaceutical complexes: a solid-state NMR approach, CrystEngComm. 13 (2011) 3213–3223. doi:10.1039/c0ce00657b.
[196] F. Pourpoint, J. Yehl, M. Li, R. Gupta, J. Trebosc, O. Lafon, J.-P. Amoureux, T. Polenova, NMR Crystallography of an Oxovanadium(V) Complex by an Approach Combining Multinuclear Magic Angle Spinning NMR, DFT, and Spin Dynamics Simulations, ChemPhysChem. 16 (2015) 1619–1626. doi:10.1002/cphc.201500033.
[197] L. Szeleszczuk, D.M. Pisklak, M. Zielinska-Pisklak, I. Wawer, Effects of structural differences on the NMR chemical shifts in cinnamic acid derivatives: Comparison of GIAO and GIPAW calculations, Chem. Phys. Lett. 653 (2016) 35–41. doi:10.1016/j.cplett.2016.04.075.
[198] T. Charpentier, The PAW/GIPAW approach for computing NMR parameters: A new dimension added to NMR study of solids, Solid State Nucl. Magn. Reson. 40 (2011) 1–20. doi:10.1016/j.ssnmr.2011.04.006.
[199] D.V. Dudenko, J.R. Yates, K.D.M. Harris, S.P. Brown, An NMR crystallography DFT-D approach to analyse the role of intermolecular hydrogen bonding and pi-pi interactions in driving cocrystallisation of indomethacin and nicotinamide, CrystEngComm. 15 (2013) 8797–8807. doi:10.1039/c3ce41240g.
[200] S.P. Brown, Hydrogen Bonding in Crystalline Organic Solids, in: R.K. Harris, R.E. Wasylishen, M.J. Duer (Eds.), NMR Crystallography, John Wiley & Sons, Ltd, Chichester, UK, 2009: pp. 321–339. doi:10.1002/9780470034590.emrstm1006.

[201] C. Gervais, C. Coelho, T. Azais, J. Maquet, G. Laurent, F. Pourpoint, C. Bonhomme, P. Florian, B. Alonso, G. Guerrero, P.H. Mutin, F. Mauri, First principles NMR calculations of phenylphosphinic acIdC(6)H(5)HPO(OH): Assignments, orientation of tensors by local field experiments and effect of molecular motion, J. Magn. Reson. 187 (2007) 131–140. doi:10.1016/j.jmr.2007.03.018.
[202] R. Dervisoglu, D.S. Middlemiss, F. Blanc, Y.-L. Lee, D. Morgan, C.P. Grey, Joint Experimental and Computational O-17 and H-1 Solid State NMR Study of Ba2In2O4(OH)(2) Structure and Dynamics, Chem. Mat. 27 (2015) 3861–3873. doi:10.1021/acs.chemmater.5b00328.
[203] J.A. Fernandes, M. Sardo, L. Mafra, D. Choquesillo-Lazarte, N. Masciocchi, X-ray and NMR Crystallography Studies of Novel Theophylline Cocrystals Prepared by Liquid Assisted Grinding, Cryst. Growth Des. 15 (2015) 3674–3683. doi:10.1021/acs.cgd.5b00279.
[204] E.D.L. Smith, R.B. Hammond, M.J. Jones, K.J. Roberts, J.B.O. Mitchell, S.L. Price, R.K. Harris, D.C. Apperley, J.C. Cherryman, R. Docherty, The determination of the crystal structure of anhydrous theophylline by X-ray powder diffraction with a systematic search algorithm, lattice energy calculations, and C-13 and N-15 solid-state NMR: A question of polymorphism in a given unit cell, J. Phys. Chem. B. 105 (2001) 5818–5826. doi:10.1021/jp002060x.
[205] F. Franco, M. Baricco, M.R. Chierotti, R. Gobetto, C. Nervi, Coupling Solid-State NMR with GIPAW ab Initio Calculations in Metal Hydrides and Borohydrides, J. Phys. Chem. C. 117 (2013) 9991–9998. doi:10.1021/jp3126895.
[206] S.J. Clark, M.D. Segall, C.J. Pickard, P.J. Hasnip, M.J. Probert, K. Refson, M.C. Payne, First principles methods using CASTEP, Z. Kristallogr. - Cryst. Mater. 220 (2005) 567–570. doi:10.1524/zkri.220.5.567.65075.
[207] H.E. Kerr, L.K. Softley, K. Suresh, A. Nangia, P. Hodgkinson, I.R. Evans, A furosemide-isonicotinamide cocrystal: an investigation of properties and extensive structural disorder, CrystEngComm. 17 (2015) 6707–6715. doi:10.1039/c5ce01183c.
[208] A. Jablonski, C.J. Powell, Relationships between electron inelastic mean free paths, effective attenuation lengths, and mean escape depths, J. Electron Spectrosc. Relat. Phenom. 100 (1999) 137–160. doi:10.1016/S0368-2048(99)00044-4.
[209] J.S. Stevens, S.J. Byard, S.L.M. Schroeder, Salt or Co-Crystal? Determination of Protonation State by X-Ray Photoelectron Spectroscopy (XPS), J. Pharm. Sci. 99 (2010) 4453–4457. doi:10.1002/jps.22164.
[210] D. Briggs, M.P. Seah, Practical Surface Analysis, Auger and X-ray Photoelectron Spectroscopy, 2nd ed., Wiley, Chichester, UK, 1990.
[211] J.S. Stevens, S.J. Byard, S.L.M. Schroeder, Characterization of Proton Transfer in Co-Crystals by X-ray Photoelectron Spectroscopy (XPS), Cryst. Growth Des. 10 (2010) 1435–1442. doi:10.1021/cg901481q.
[212] J.S. Stevens, S.L.M. Schroeder, Quantitative analysis of saccharides by X-ray photoelectron spectroscopy, Surf. Interface Anal. 41 (2009) 453–462. doi:10.1002/sia.3047.
[213] Y. Song, D. Zemlyanov, X. Chen, H. Nie, Z. Su, K. Fang, X. Yang, D. Smith, S. Byrn, J.W. Lubach, Acid–Base Interactions of Polystyrene Sulfonic Acid in Amorphous Solid Dispersions Using a Combined UV/FTIR/XPS/ssNMR Study, Mol. Pharmaceutics. 13 (2016) 483–492. doi:10.1021/acs.molpharmaceut.5b00708.
[214] J.S. Stevens, S.J. Byard, E. Zlotnikov, S.L.M. Schroeder, Detection of Free Base Surface Enrichment of a Pharmaceutical Salt by X-ray Photoelectron Spectroscopy (XPS), J. Pharm. Sci. 100 (2011) 942–948. doi:10.1002/jps.22334.
[215] C.R. Hopkins, ACS Chemical Neuroscience Molecule Spotlight on Valdoxen, ACS Chem. Neurosci. 1 (2010) 772–773. doi:10.1021/cn100062j.
[216] Y. Yan, J.-M. Chen, N. Geng, T.-B. Lu, Improving the Solubility of Agomelatine via Cocrystals, Cryst. Growth Des. 12 (2012) 2226–2233. doi:10.1021/cg201423q.

[217] R. Prohens, R. Barbas, A. Portell, M. Font-Bardia, X. Alcobe, C. Puigjaner, Polymorphism of Cocrystals: The Promiscuous Behavior of Agomelatine, Cryst. Growth Des. 16 (2016) 1063–1070. doi:10.1021/acs.cgd.5b01628.
[218] E. Skorepova, M. Husak, L. Ridvan, M. Tkadlecova, J. Havlicek, M. Dusek, Iodine salts of the pharmaceutical compound agomelatine: the effect of the symmetric H-bond on amide protonation, Crystengcomm. 18 (2016) 4518–4529. doi:10.1039/c6ce00304d.
[219] P. Sanphui, L. Rajput, S.P. Gopi, G.R. Desiraju, New multi-component solid forms of anti-cancer drug Erlotinib: role of auxiliary interactions in determining a preferred conformation, Acta Crystallogr., Sect. B: Struct. Sci., Cryst. Eng. Mat. 72 (2016) 291–300. doi:10.1107/S2052520616003607.
[220] D. Rodriguez-Barrientos, A. Rojas-Hernandez, A. Gutierrez, R. Moya-Hernandez, R. Gomez-Balderas, M. Teresa Ramirez-Silva, Determination of pK(a) values of tenoxicam from H-1 NMR chemical shifts and of oxicams from electrophoretic mobilities (CZE) with the aid of programs SQUAD and HYPNMR, Talanta. 80 (2009) 754–762. doi:10.1016/j.talanta.2009.07.058.
[221] J.R. Patel, R.A. Carlton, T.E. Needham, C.O. Chichester, F.G. Vogt, Preparation, structural analysis, and properties of tenoxicam cocrystals, Int. J. Pharm. 436 (2012) 685–706. doi:10.1016/j.ijpharm.2012.07.034.
[222] M. Caira, L. Nassimbeni, M. Timme, Zwitterionic Nature of Tenoxicam - Crystal-Structures and Thermal Analyses of a Polymorph of Tenoxicam and a 1/1 Tenoxicam/Acetonitrile Solvate, J. Pharm. Sci. 84 (1995) 884–888. doi:10.1002/jps.2600840719.
[223] Kim, Y. B, Kwon, Y. H., Park, I. Y., Lee, B. J., Kim, C.-K., The crystal structure of tenoxicam (C 13 H 11 N 3 O 4 S 2), a non-steroidal antiinflammatory agent., Seoul. Univ. J. Pharm. Sci. 18 (1993) 1–12.
[224] G. Bolla, P. Sanphui, A. Nangia, Solubility Advantage of Tenoxicam Phenolic Cocrystals Compared to Salts, Cryst. Growth Des. 13 (2013) 1988–2003. doi:10.1021/cg4000457.
[225] P.K. Goswami, R. Thaimattam, A. Ramanan, Multiple Crystal Forms of p-Aminosalicylic Acid: Salts, Salt Co-Crystal Hydrate, Co-Crystals, and Co-Crystal Polymorphs, Cryst. Growth Des. 13 (2013) 360–366. doi:10.1021/cg3015332.
[226] G. Verreck, A. Decorte, K. Heymans, J. Adriaensen, D. Liu, D. Tomasko, A. Arien, J. Peeters, G. Van den Mooter, M.E. Brewster, Hot stage extrusion of p-amino salicylic acid with EC using CO2 as a temporary plasticizer, Int. J. Pharm. 327 (2006) 45–50. doi:10.1016/j.ijpharm.2006.07.024.
[227] V. Andre, M.T. Duarte, D. Braga, F. Grepioni, Polymorphic Ammonium Salts of the Antibiotic 4-Aminosalicylic Acid, Cryst. Growth Des. 12 (2012) 3082–3090. doi:10.1021/cg300284z.
[228] S.L. Morissette, Ö. Almarsson, M.L. Peterson, J.F. Remenar, M.J. Read, A.V. Lemmo, S. Ellis, M.J. Cima, C.R. Gardner, High-throughput crystallization: polymorphs, salts, co-crystals and solvates of pharmaceutical solids, Adv. Drug Delivery Rev. 56 (2004) 275–300. doi:10.1016/j.addr.2003.10.020.
[229] L.S. Reddy, S.J. Bethune, J.W. Kampf, N. Rodriguez-Hornedo, Cocrystals and Salts of Gabapentin: pH Dependent Cocrystal Stability and Solubility, Cryst. Growth Des. 9 (2009) 378–385. doi:10.1021/cg800587y.
[230] G. He, P.S. Chow, R.B.H. Tan, Predicting Multicomponent Crystal Formation: The Interplay between Homomeric and Heteromeric Interactions, Cryst. Growth Des. 9 (2009) 4529–4532. doi:10.1021/cg900538g.
[231] P. Grobelny, A. Mukherjee, G.R. Desiraju, Drug-drug co-crystals: Temperature-dependent proton mobility in the molecular complex of isoniazid with 4-aminosalicylic acid, CrystEngComm. 13 (2011) 4358–4364. doi:10.1039/c0ce00842g.
[232] J.-R. Dai, Y.-Z. Li, W. Wang, Y.-T. Xing, G.-L. Qu, Y.-S. Liang, Resistance to niclosamide in Oncomelania hupensis, the intermediate host of Schistosoma japonicum: should we be worried?, Parasitology. 142 (2015) 332–340. doi:10.1017/S0031182014000870.

[233] B.I. Harriss, C. Wilson, I.R. Evans, Niclosamide methanol solvate and niclosamide hydrate: structure, solvent inclusion mode and implications for properties, Acta Crystallogr. Sect. C-Struct. Chem. 70 (2014) 758-U86. doi:10.1107/S2053229614015496.
[234] P. Sanphui, S.S. Kumar, A. Nangia, Pharmaceutical Cocrystals of Niclosamide, Cryst. Growth Des. 12 (2012) 4588–4599. doi:10.1021/cg300784v.
[235] F. Fischer, M.U. Schmidt, S. Greiser, F. Emmerling, The challenging case of the theophylline-benzamide cocrystal, Acta Crystallogr., Sect. C: Struct. Chem. 72 (2016) 217–224. doi:10.1107/S2053229616002643.
[236] D. Braga, F. Grepioni, L. Maini, G.I. Lampronti, D. Capucci, C. Cuocci, Structure determination of novel ionic co-crystals from powder data: the use of rigid fragments in simulated annealing algorithms, CrystEngComm. 14 (2012) 3521–3527. doi:10.1039/c2ce25057h.
[237] T.T. Ong, P. Kavuru, T. Nguyen, R. Cantwell, L. Wojtas, M.J. Zaworotko, 2:1 Cocrystals of Homochiral and Achiral Amino Acid Zwitterions with Li+ Salts: Water-Stable Zeolitic and Diamondoid Metal-Organic Materials, J. Am. Chem. Soc. 133 (2011) 9224–9227. doi:10.1021/ja203002w.
[238] D. Braga, F. Grepioni, V. Andre, M.T. Duarte, Drug-containing coordination and hydrogen bonding networks obtained mechanochemically, CrystEngComm. 11 (2009) 2618–2621. doi:10.1039/b913433f.
[239] J. Wouters, F. Grepioni, D. Braga, R.M. Kaminski, S. Rome, L. Aerts, L. Quere, Novel pharmaceutical compositions through co-crystallization of racetams and Li+ salts, CrystEngComm. 15 (2013) 8898–8902. doi:10.1039/c3ce41539b.
[240] G.R. Desiraju, P.S. Ho, L. Kloo, A.C. Legon, R. Marquardt, P. Metrangolo, P. Politzer, G. Resnati, K. Rissanen, Definition of the halogen bond (IUPAC Recommendations 2013), Pure Appl. Chem. 85 (2013) 1711–1713. doi:10.1351/PAC-REC-12-05-10.
[241] M. Baldrighi, D. Bartesaghi, G. Cavallo, M.R. Chierotti, R. Gobetto, P. Metrangolo, T. Pilati, G. Resnati, G. Terraneo, Polymorphs and co-crystals of haloprogin: an antifungal agent, CrystEngComm. 16 (2014) 5897–5904. doi:10.1039/C4CE00367E.
[242] M. Baldrighi, G. Cavallo, M.R. Chierotti, R. Gobetto, P. Metrangolo, T. Pilati, G. Resnati, G. Terraneo, Halogen Bonding and Pharmaceutical Cocrystals: The Case of a Widely Used Preservative, Mol. Pharmaceutics. 10 (2013) 1760–1772. doi:10.1021/mp300574j.
[243] G. Resnati, P. Metrangolo, G. Terraneo, M. Baldrighi, Co-Crystals of 3-Iodopropynyl Butylcarbamate, US2015051280 (A1), 2015. https://worldwide.espacenet.com/publicationDetails/biblio?FT=D&date=20150219&DB=EPODOC&locale=en_EP&CC=US&NR=2015051280A1&KC=A1&ND=4 (accessed March 2, 2017).
[244] A.E. Wakeling, S.P. Guy, J.R. Woodburn, S.E. Ashton, B.J. Curry, A.J. Barker, K.H. Gibson, ZD1839 (Iressa): An orally active inhibitor of epidermal growth factor signaling with potential for cancer therapy, Cancer Res. 62 (2002) 5749–5754.
[245] N.R. Goud, S. Gangavaram, K. Suresh, S. Pal, S.G. Manjunatha, S. Nambiar, A. Nangia, Novel furosemide cocrystals and selection of high solubility drug forms, J. Pharm. Sci. 101 (2012) 664–680. doi:10.1002/jps.22805.
[246] S.H. Thorat, S.K. Sahu, M.V. Patwadkar, M.V. Badiger, R.G. Gonnade, Drug-Drug Molecular Salt Hydrate of an Anticancer Drug Gefitinib and a Loop Diuretic Drug Furosemide: An Alternative for Multidrug Treatment, J. Pharm. Sci. 104 (2015) 4207–4216. doi:10.1002/jps.24651.